

robust circadian expression of *Per2* in the cell-autonomous clock.

MATERIALS AND METHODS

Cell culture

Mouse fibroblast NIH3T3 cells were cultured in Dulbecco's modified Eagle's medium (DMEM) supplemented with 10% fetal bovine serum (FBS) and a mixture of penicillin and streptomycin at 37°C under a humidified 5% CO₂ atmosphere.

Small interfering RNA (siRNA)

We designed E4BP4 siRNA for knockdown experiments using BLOCK-iTTM RNAi Designer (<https://rnaidesigner.invitrogen.com/rnaiexpress/>), and BLOCK-iT Fluorescent Oligo (Invitrogen) served as a control. These oligonucleotides were introduced into NIH3T3 cells at a final concentration of 10 nM using X-treamGENE (Roche Diagnostics) or Lipofectamine 2000 (Invitrogen) according to the suppliers' protocols.

Western blotting

NIH3T3 cells were transfected with the expression vectors, Myc-tagged E4BP4 or Myc-tagged HLF after siRNA manipulation. After a 24 h incubation, proteins were separated on 10% SDS-PAGE gels (31) and transferred to nitrocellulose membranes (Bio-Rad). After blocking nonspecific binding with 3% dry milk in PBS, proteins were probed with anti-Myc monoclonal antibody (clone 9E10; Roche Diagnostics) and then incubated with a horseradish peroxidase-conjugated anti-mouse IgG (Upstate). Immunoreactive proteins were visualized using ECL (Amersham Biosciences) according to the manufacturer's instructions. The same membrane was reprobed with anti-actin antibody (clone C4, CHEMICOM).

Northern blotting

Total RNA was prepared using ISOGEN (Nippon Gene) and then poly(A)⁺ RNA was purified using a GenElute mRNA Miniprep Kit (Sigma-Aldrich). Northern blotting proceeded as described (32). Probes labeled with ³²P were generated from cDNA fragments of *Per2* (bases 1123–1830; GenBank accession no. AF036893), *E4BP4* (bases 61–770; GenBank accession no. U83148), *Bmali* (bases 231–910; GenBank accession no. AF015953) and β-actin. The relative expression level of each gene to that of β-actin was calculated using Image Gauge (FUJIFILM).

Real-time luciferase assay

Fragments of DNA containing the *Per2* promoter region and its derivatives were cloned into pGL3-dLuc that contains a rapid degradation domain modified from mouse ornithine decarboxylase at the carboxy-terminal end of firefly luciferase (33). After transfecting reporter plasmids using PolyFect (Qiagen), NIH3T3 cells were stimulated with 100 nM dexamethasone for 2 h and then incubated with DMEM containing 0.1 mM luciferin (Promega), 25 mM HEPES (pH 7.2) and 10% FBS. Bioluminescence was measured and integrated

for 1 min at intervals of 10 min using Kronos AB-2500 (ATTO).

Transient luciferase assay

The *Per2* promoter region containing E4BP4-binding sites and its derivatives were cloned into pGL3-Basic vector (Promega). The constructs were co-transfected with phRG-TK (Promega) as an internal control into NIH3T3 cells. Luciferase activities were measured using the Dual-Luciferase Reporter Assay System (Promega) and a Luminometer Model TD-20/20 (Turner Designs). The transcriptional activities were normalized relative to *Renilla* luciferase activities.

Gel shift assay

Gel shifts were examined as described (34). Briefly, nuclear extracts were purified from NIH3T3 cells using CellLytic NucLEAR EXTRACTION KIT (Sigma). Recombinant E4BP4 was purchased from ABNOVA. The probes (A-site, from -251 to -92; B-site, from +112 to +332 of *mPer2*) were amplified using the following primer sets: A-site, 5'-GGAAGTGGACGCCCTACTCG-3' (forward) and 5'-CGAACCTGAGAGCTACGCTC-3' (reverse); B-site, 5'-TTGACCGCGGCGAACGGTGAGTG-3' (forward) and 5'-GGGACGCAGTGTGAACCTGG-3' (reverse). Nucleotide sequences of the 16-bp oligonucleotide probes for the A- and B-sites were 5'-CGTCTTATGTAAAGAG-3' and 5'-CGTCTTACGTAAACCGG-3', respectively. These probes were end-labeled with [γ -³²P]ATP using T4 polynucleotide kinase (New England BioLabs). The DNA probes were suspended in 10 μ l of 16 mM HEPES (pH 7.5), 150 mM KCl, 16% (v/v) glycerol, 1.6 mM MgCl₂, 0.8 mM dithiothreitol, 0.4 mM PMSF, 1 mM EDTA, 0.8 mg/ml BSA, 0.06 mg/ml poly(dI-dC) and 0.01% NP-40 in the presence of or absence of competitor oligonucleotides and incubated with the nuclear extracts or E4BP4 protein. The anti-E4BP4 antibody was also added for super-shift assays. The samples were resolved by electrophoresis on 4% polyacrylamide gels in 40 mM Tris-acetate, 1 mM EDTA and 5% glycerol at 110 V for 2 h.

Chromatin immunoprecipitation (ChIP) assay

Assays of ChIP proceeded as described (34). Briefly, NIH3T3 cells were cross-linked with 1% formaldehyde for 15 min at room temperature and then washed twice with ice-cold PBS. The cells were shattered with lysis buffer (25 mM Tris-HCl (pH 8.0), 140 mM NaCl, 1% Triton X-100, 0.1% SDS, 3 mM EDTA and 1 mM PMSF) on ice for 30 min. Sonication to shear DNA into 100–300 bp fragments was followed by centrifugation and supernatants containing soluble chromatin were collected. The chromatin fraction was incubated with anti-E4BP4 antibody (E-16, Santa Cruz Biotechnology) overnight at 4°C, followed by salmon sperm DNA/protein G agarose (Upstate). Chromatin immunocomplexes were washed three times, once with wash buffer 1 (20 mM Tris-HCl (pH 8.0), 150 mM NaCl, 0.1% SDS, 1% Triton X-100 and 2 mM EDTA), once with wash buffer 2 (20 mM Tris-HCl (pH 8.0), 500 mM NaCl, 0.1% SDS, 1% Triton X-100 and 2 mM EDTA) and once with wash buffer 3 (10 mM Tris-HCl (pH 8.0), 0.25 M LiCl, 1% Nonidet P-40, 1%

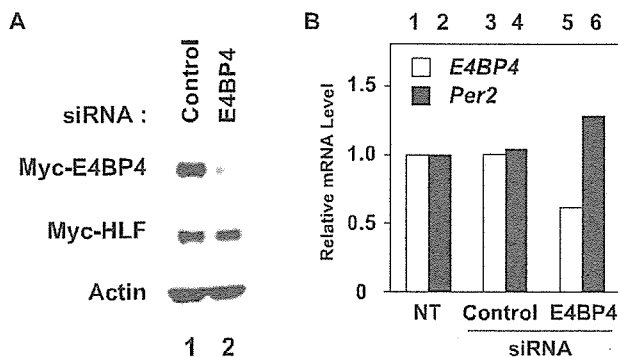


Figure 1. E4BP4 is a negative regulator of *Per2* transcription. (A) RNA interference with E4BP4. NIH3T3 cells were transfected with scrambled siRNA (Control siRNA) or specific siRNA for E4BP4 (E4BP4 siRNA). Myc-tagged E4BP4 was co-transfected with Myc-tagged HLF (as a negative control) 24 h later. At 48 h after siRNA transfection, the E4BP4 protein level was determined by Western blotting using anti-Myc antibody. The same membrane was stripped and reprobed with anti-actin antibody. (B) Knockdown of E4BP4 increased *Per2* transcription. NIH3T3 cells transfected with siRNAs (Control siRNA or E4BP4 siRNA) or non-transfected (NT) were analyzed for *E4BP4* and *Per2* mRNA by Northern blotting. Poly(A)⁺ RNA was purified from total RNA of two independent experiments. Expression levels were normalized to those of β -actin. Values are relative to that of NT cells.

deoxycholate and 1 mM EDTA). All washes proceeded at 4°C for 5 min. The samples were then washed twice with TE buffer. The immunocomplexes were removed with 1% SDS and 0.1 M NaHCO₃ and then heated overnight at 65°C to reverse the crosslinks. The crosslinks of DNA input samples were similarly reversed. Sample DNA was purified and then putative E4BP4 target regions (A-site, from -251 to -92; B-site, from +112 to +332 of mPer2) were amplified by PCR using the following primer sets: A-site, 5'-GGAAGTGGACGCG-CCTACTCG-3' (forward) and 5'-CGAACCTGAGAGCT-ACGCTC-3' (reverse); B-site, 5'-TTGACGCGGGGAAGCG-GTGAGTG-3' (forward) and 5'-GGGACGCAGTGTGAAC-CTGG-3' (reverse).

RESULTS

E4BP4 down-regulates *Per2* transcription

E4BP4 is a mammalian homologue of *vrille* (*vri*) that functions as a key negative component of the *Drosophila* circadian clock (12,26,27). However, whether or not E4BP4 is required for mammalian circadian clocks remains unclear. We initially examined the effect of E4BP4 upon *Per2* transcription. To determine whether E4BP4 regulates *Per2* gene expression, we performed knockdown experiments using small interfering RNA (siRNA) for *E4BP4* (E4BP4 siRNA). The induction of E4BP4 siRNA into NIH3T3 cells resulted in a significant decrease in the protein level of exogenously expressed Myc-tagged E4BP4, whereas the level of Myc-tagged Hepatic Leukemia Factor (HLF) was not affected (Figure 1A, lane 2), suggesting that the siRNA specifically knocked down E4BP4. We then examined the mRNA levels of *E4BP4* and *Per2* by Northern blotting. After introducing E4BP4 siRNA into NIH3T3 cells, the mRNA level of endogenous *E4BP4* decreased to ~60% of that in non-transfected (NT) cells (Figure 1B, lane 5). On the other

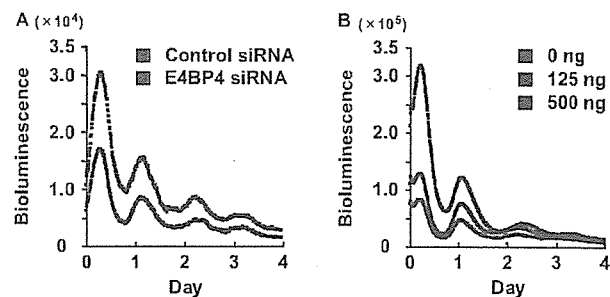


Figure 2. E4BP4 negatively regulates *Per2* oscillation in cell-autonomous clock. (A) Effect of E4BP4-knockdown by siRNA. B, Effect of E4BP4-overexpression. Promoter region of *mPer2* (-798 to +331 relative to the cap site) was examined in real-time reporter gene assays. After introduction of siRNAs (A) or E4BP4-expression vector (B), bioluminescence was measured and integrated for 1 min at intervals of 10 min. The results are representative of three independent experiments.

hand, that of *Per2* increased to ~130% of that in NT cells (Figure 1B, lane 6). The levels of neither *E4BP4* mRNA (Figure 1B, lane 3) nor *Per2* mRNA (Figure 1B, lane 4) were affected by induction with scrambled siRNA (Control siRNA). These results suggest that E4BP4 suppresses *Per2* transcription.

The circadian clock is cell-autonomous (35,36). Circadian oscillators are located not only in the suprachiasmatic nucleus (SCN) of the brain, which is the central circadian pacemaker in mammals, but also in most peripheral tissues (19,37,38) and even in established cell lines (39). To examine the role of E4BP4 on the circadian expression of *Per2* in the cell-autonomous clock, we performed real-time luciferase assays (33,40) in NIH3T3 cells using the reporter plasmid containing the *mPer2* (-798 to +331) promoter to drive destabilized luciferase (*mPer2-dLuc*). The transcriptional start site (TSS) is indicated as +1 (24). After the introduction of E4BP4 siRNA, the cells were transfected with *mPer2-dLuc* and circadian gene expression was induced with 100 nM dexamethasone (41). We measured bioluminescence in the presence of luciferin and integrated signals for 1 min at intervals of 10 min. As reported (24,25,30), the transcriptional fluctuation from *mPer2-dLuc* showed robust circadian oscillation. The induction of E4BP4 siRNA caused a remarkable overall 1.86-fold increase in the transcriptional activity of *mPer2-dLuc* compared with Control siRNA (Figure 2A). Conversely, exogenously expressed E4BP4 resulted in a gradual reduction in the circadian expression of *Per2* (Figure 2B). These results suggested that E4BP4 functions as a negative regulator of *Per2* oscillation in the cell-autonomous clock.

Two putative E4BP4-binding sites on the *Per2* promoter region

Although many putative E4BP4-binding sites are located in clock and clock-related genes (30), whether the E4BP4-mediated negative regulation of *Per2* is direct or indirect remains unknown. To examine whether E4BP4 directly represses the transcriptional activity of *Per2*, we searched the mouse *Per2* promoter region and genomic gene sequences for the E4BP4-binding site, RT(G/T)AYGTAAY (where R is a purine and Y is a pyrimidine) (42). Sequence analysis

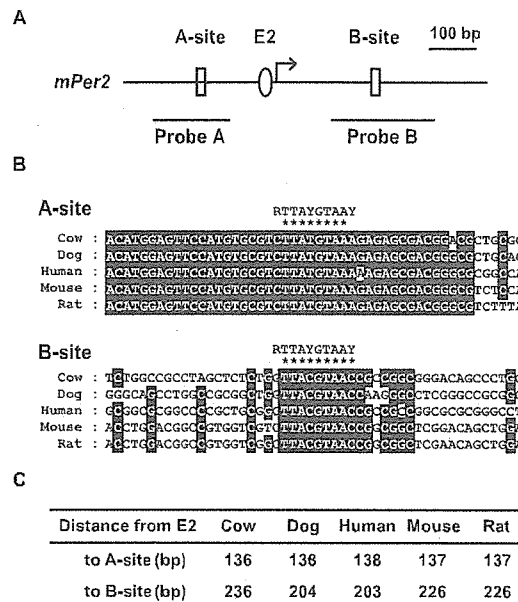


Figure 3. Two putative E4BP4-binding sites on mammalian *Per2* promoter regions. (A) Maps of *mPer2* promoter region. Arrow and oval indicate transcription start site (TSS) and E2 enhancer (position at -20 relative to cap site) (24), respectively. Two putative E4BP4-binding sites are shown as open boxes. Positions of probes used for gel shift analysis are indicated as horizontal bars. (B) Sequence alignment of region around E4BP4-binding sites. Conserved sequences are shown as white characters on black. Consensus E4BP4-binding sequences are shown above and identical bases are indicated by asterisks. (C) Distance between putative E4BP4-binding sites and E2.

revealed two putative E4BP4-binding sites (termed A-site at -151 and B-site at +197) around the TSS (Figure 3A). The nucleotide sequences of the A- and B-sites matched 8/10 and 9/10 bp of the consensus E4BP4-binding sequence, respectively. Further analysis revealed that the nucleotide sequence around the A-site is highly conserved among mammalian *Per2* promoter regions (cow, dog, human, mouse and rat) (Figure 3B, upper panel). On the other hand, a B-site is located at a diverse region of intron 1 (Figure 3B, lower panel). Interestingly, the location of both sites with respect to the E2 enhancer was highly conserved beyond species (Figure 3C). These data suggest that the A- and B-sites are functionally important for the E4BP4-mediated negative regulation of *Per2*.

E4BP4 directly represses the transcriptional activity of *Per2* through the B-site

To understand the functional importance of the A- and B-sites for E4BP4-mediated transcriptional repression of *Per2*, we performed luciferase assays with mutant constructs of the *mPer2* (-798 to +331) promoter (Figure 4A) to prevent E4BP4 binding (Supplementary Figure S1). The mutated sequences of the A- and B-sites were 5'-CCAGTGTAAA-3' and 5'-CCAGCGTAAC-3', respectively (43). E4BP4-mediated transcriptional repression of these mutant constructs was examined, and normalized expression level was calculated relative to the luciferase activity in the absence of E4BP4. Consistent with the observations in Figure 2B,

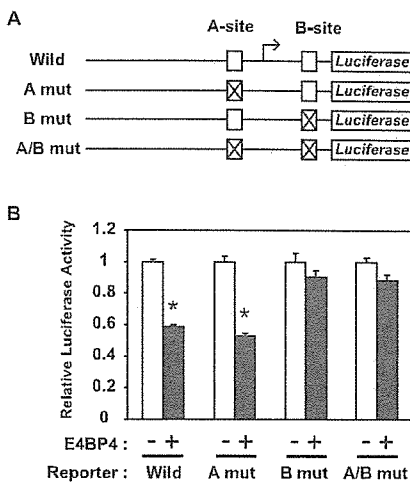


Figure 4. B-site is responsible for E4BP4-mediated transcriptional repression of *Per2*. (A) Schematic representation of mutant constructs of *mPer2* promoter. Arrow indicates TSS. Open boxes, putative E4BP4-binding sites. Each or both of the putative E4BP4-binding sites were mutated (A-site, 5'-CTTATGTAAA-3' to 5'-CCAGTGTAAA-3'; B-site, 5'-CTTACGTAAAC-3' to 5'-CCAGCGTAAC-3'). (B) Analysis of E4BP4-binding sites on *Per2* promoter. Transcriptional assay was performed with indicated mutant constructs. E4BP4 expression plasmid is present (+) or absent (-). Normalized expression level was calculated relative to luciferase activity in absence of E4BP4. Values are means \pm SEM of three replicates from a single assay. (*) Significant difference between presence versus absence of E4BP4 ($P < 0.001$). Results are representative of two independent experiments.

exogenously expressed E4BP4 repressed the transcriptional activity of the wild type of *mPer2* (-798 to +331) promoter (Wild, % of repression by E4BP4 was 41.0%). A mutation of the A-site (A mut; 47.2%) resulted in the same transcriptional repression as with the Wild type. However, mutation of the B-site (B mut; 9.67%) and of both the A- and B-sites (A/B mut; 11.7%) recovered from the repression (Figure 4B). Similar results were obtained using deletion constructs of E4BP4-binding sites (data not shown). As the PAR transcription factors (DBP, HLF and TEF) are known to bind to the identical nucleotide sequence as E4BP4 *in vitro* (29,30), we also examined the effect of DBP, HLF and TEF on the *mPer2* promoter activity using same mutant and deletion constructs. However, neither the A- nor B-site was responsible for the transcriptional activation of *mPer2* by these PAR transcription factors (Supplementary Figure S2). These results suggest that the B-site is functionally important for the E4BP4-mediated transcriptional repression of *Per2*.

To clarify the importance of the B-site for E4BP4-mediated transcriptional repression of the *Per2* promoter through the DNA-binding activity of E4BP4, we performed gel shift assays using nuclear extracts from the NIH3T3 cells expressing Myc-tagged E4BP4 and the probes shown in Figure 3A. We used end-labeled DNA fragments of \sim 200 bp containing either the A- or the B-site probes (Figure 3A). We observed shifted bands for both probes and the bands disappeared in the presence of an unlabeled competitor containing the consensus E4BP4-binding sequence, indicating that the protein-DNA complexes were specific for the E4BP4-binding site (Figure 5A, asterisk in probe A and double asterisk in probe B). However, the

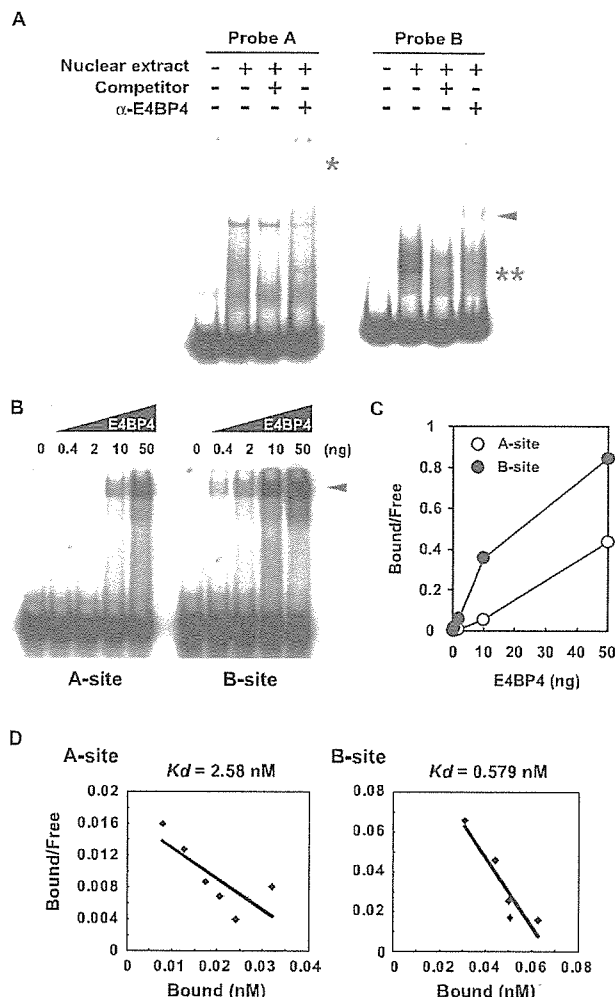


Figure 5. E4BP4 preferentially binds to B-site *in vitro*. (A) Gel shift analysis using nuclear extracts from NIH3T3 cells transfected with the E4BP4-expression vector. Positions of probes A and B are shown in Figure 3A and competing nucleotide sequence is 5'-TCGAGAAAAAAATTATGT-AACGGTC-3'. * and **, band specifically bound to E4BP4-binding site; arrowhead, supershifted band. The band specifically bound to E4BP4-binding site in probe B (**) not but in probe A (*) was supershifted with an anti-E4BP4 antibody. (B) Gel shift analysis using recombinant-E4BP4. Oligonucleotide probes (A-site, 5'-CGTCCTATGTAAAGAG-3'; B-site, 5'-CGTCTTACGTAAACCGG-3') were incubated with increasing amounts of recombinant-E4BP4 (0, 0.4, 2, 10 and 50 ng). Arrowhead, band bound to E4BP4. (C) Quantification of E4BP4-oligonucleotide probe complex. (D) Determination of K_d s for binding of recombinant-E4BP4 to A- and B-sites. Recombinant-E4BP4 (10 ng) was incubated with increasing amounts of radiolabeled 16-bp core probes for A- and B-sites. After gel electrophoresis and autoradiography, radioactive bands corresponding to the bound and free forms were quantified. Concentration of bound probe was plotted against total input probe to show saturation curves. K_d values were determined from these data on Scatchard plots. Slope of best-fit line is equal to $-1/K_d$.

supershifted band with an anti-E4BP4 antibody was observed in only probe B (Figure 5A, arrowhead). This was also confirmed using an anti-Myc antibody (data not shown). These results suggest that E4BP4 binds to the B-site and forms a DNA-protein complex. We questioned why only the probe B (double asterisk) showed a supershifted band. Figure 3B

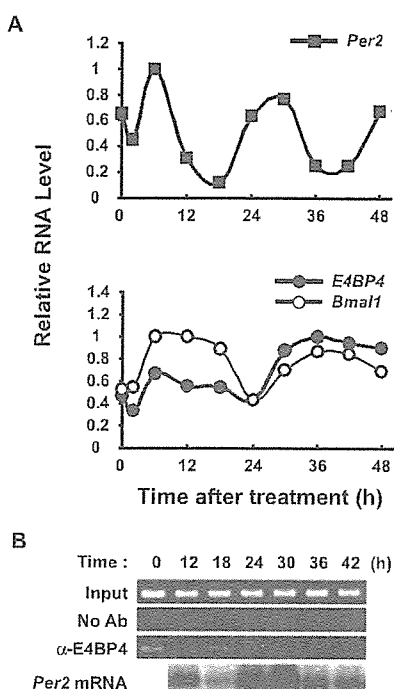


Figure 6. Binding of E4BP4 correlates with negative *Per2* regulation. (A) *E4BP4* transcript shows anti-phase to *Per2* oscillation. NIH3T3 cells were stimulated with 100 nM dexamethasone, and mRNA was analyzed by northern blotting. Levels of RNA were normalized to β -actin expression and peak values of individual curves were set to 1. (B) Oscillatory binding of E4BP4 to *Per2* promoter *in vivo*. NIH3T3 cells were stimulated with dexamethasone and ChIP assays of B-sites were applied. Bottom panel, *Per2* mRNA oscillation. No Ab, without antibody; α -E4BP4, with anti-E4BP4 antibody.

shows that the nucleotide sequences of A- and B-sites were not identical. Therefore, we examined the affinity of E4BP4 for the A- and B-sites using gel shift assays, with recombinant-E4BP4 protein and 16-bp core probes for each site. Figure 5B and C shows that the B-site had higher affinity than the A-site for E4BP4. Further analysis determined that the K_d s for binding of the recombinant-E4BP4 to the A- and B-sites were 2.58 and 0.579 nM, respectively (Figure 5D). These results indicated that E4BP4 preferentially binds to the B-site rather than to the A-site *in vitro*.

We then performed ChIP assays in NIH3T3 cells expressing Myc-tagged E4BP4 to determine the situation *in vivo*. Consistent with the observations in Figure 5 *in vitro*, the ChIP assays also suggested that E4BP4 binds to the B-site much more than to the A-site on the *Per2* promoter *in vivo* (data not shown). Taken together, these results indicated that E4BP4 directly represses *Per2* transcription via the B-site on the promoter.

Binding of E4BP4 correlates with negative regulation of *Per2*

The circadian expression of E4BP4 is similar to that of the anti-phase to *Per2* oscillations in both the SCN and the liver (29,33). We therefore postulated that E4BP4 plays an important role in *Per2* oscillation in the cell-autonomous

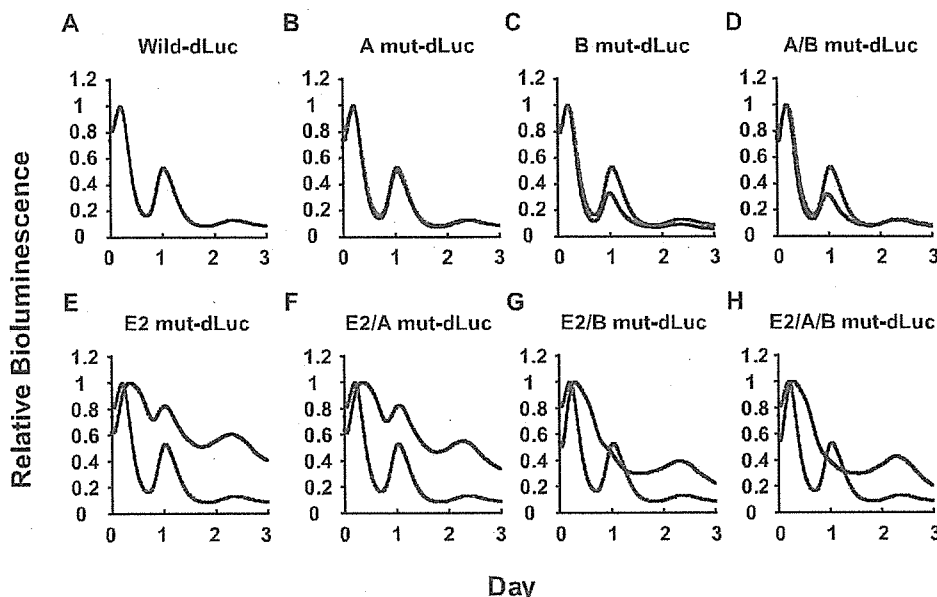


Figure 7. (A–H) B-site drives the circadian expression of *Per2*. NIH3T3 cells were transfected with indicated mutant constructs, incubated with dexamethasone and then bioluminescence was measured. For accurate comparison, light gray dots show bioluminescence from Wild-dLuc. Peak values of individual curves were set to 1. Results are representative of three independent experiments that generated similar results. Wild, wild type *mPer2* promoter; A mut, mutated A-site; B mut, mutated B-site; E2 mut, mutated E2 enhancer (5'-GCTAGT-3').

core clock. To test this hypothesis, we analyzed the temporal expression profile of *E4BP4* mRNA in NIH3T3 cells after stimulation with 100 nM dexamethasone (44). Northern blots showed rhythmic *E4BP4* mRNA expression with a peak at 36 h and a trough at 24 h, an anti-phase to *Per2* oscillation and a similar phase to *Bmiall* oscillation (Figure 6A). We then examined the temporal binding of endogenous *E4BP4* on the *Per2* promoter by ChIP analysis. The ChIP assay showed that the peak of endogenous *E4BP4* binding to the *Per2* promoter almost matched the trough of *Per2* mRNA expression (Figure 6B; see 18 and 36 h). The correlation between the binding activity of *E4BP4* and the transcriptional repression of *Per2* suggests that *E4BP4* plays an important role as a negative regulator for the circadian expression of *Per2* in the cell-autonomous core clock.

B-site is responsible for the generation of high amplitude in *Per2* oscillation

To clarify the role of *E4BP4* binding in *Per2* mRNA oscillation in the circadian clock, we performed real-time reporter assays using mutants of the A- and B-sites. Circadian oscillation of the construct with the wild type of *mPer2* promoter (Wild-dLuc) was obvious (Figure 7A). Superimposing the oscillation profile of the mutant construct of the A-site (A mut-dLuc) on that of the wild type, confirmed that both oscillation profiles were similar, indicating that the A-site is not prerequisite for the circadian expression of *Per2* (Figure 7B). On the other hand, the amplitude of oscillation by mutants of the B-site (B mut-dLuc) and of both the A- and B-sites (A/B mut-dLuc) was lower than that of Wild-dLuc (Figure 7C and D). These findings suggest that the B-site is responsible for generating the high amplitude of *Per2* oscillation.

Binding of *E4BP4* to the B-site is required for circadian expression of *Per2*

The E2 enhancer is required for *Per2* oscillation, which is mediated by CLOCK:BMAL1 and it is located 226 bp upstream of the B-site (24,25). To understand the relationship between the E2 enhancer and the B-site for *Per2* oscillation, we performed real-time reporter assays using mutants of the E2 enhancer that lack transcriptional activation by CLOCK:BMAL1 (Supplementary Figure S3) (24). Surprisingly, the mutant of the E2 enhancer (E2 mut-dLuc), which contains both of the intact *E4BP4* sites, retained the ability to potently drive the circadian oscillation of *Per2* (Figure 7E), whereas the circadian rhythmicity for the mutant of the E2 enhancer and the B-site (E2/B mut-dLuc) as well as the mutant of the E2 enhancer and the A/B-sites (E2/A/B mut-dLuc) was lost (Figure 7G and H). The mutant of both the E2 enhancer and the A-site (E2/A mut-dLuc) retained a clear oscillatory profile but it was subtly changed as compared with E2 mut-dLuc (Figure 7F). These results strengthened the notion that not only the E2 enhancer, but also the B-site for *E4BP4* binding is critical for the circadian expression of *Per2* mRNA in the cell-autonomous core clock.

DISCUSSION

E4BP4 is a mammalian homologue of *vrille* (*vri*) that functions as a key negative component of the *Drosophila* circadian clock (12,26,27). *E4BP4* in chickens probably plays an important role in the phase-delaying process as a light-dependent suppressor of *cPer2* (28). *E4BP4* is rhythmically expressed in mammals with an anti-phase to *Period1* (*Per1*) oscillation in the liver and the SCN and exogenously expressed *E4BP4* directly represses the *Per1* promoter

activity (29). These results indicated that E4BP4 functions as a key negative component of mammalian circadian clocks such as in *Drosophila*. However, no direct evidence has supported this notion until now. This study is the first to demonstrate that endogenous E4BP4 negatively regulates *Per2* transcription in mammals (Figure 1B), which is consistent with findings that E4BP4 represses the transcription of several genes (42,43,45). This was also confirmed in *mPer2* oscillatory transcription (Figure 2A). Figure 2 shows that the modulation of E4BP4 expression remarkably affected the amplitude, but not the period during *mPer2* oscillation. An *mPer2* mutant displays a short-circadian period followed by a loss of circadian rhythmicity in constant darkness (20), and our data also indicated a subtle elongation and shortening of the period induced by down- and up-regulated E4BP4 expression, respectively (Figure 2). The effect upon the period of oscillation might depend on the expression level and a distinguishing change in E4BP4 expression might be required. These results show that E4BP4 is involved in the circadian expression of *Per2*, which is one of the essential components of mammalian circadian clocks.

We identified two putative E4BP4-binding sites on the *Per2* promoter region (Figure 3). Ueda *et al.* described the A-site as an E4BP4-binding site that can oscillate SV40 promoter activity in a similar phase to *Per2* in established cell lines (30). Because the nucleotide sequence around the A-site is highly conserved, the A-site has simply been thought to play an important role. In this study, we showed that the novel E4BP4-binding site, the B-site, is required for the robust circadian expression of *Per2* (Figures 4 and 7). Furthermore, the importance of B-sites for E4BP4-mediated transcriptional repression of *Per2* is confirmed by the DNA-binding activity of E4BP4 *in vitro* and *in vivo* (Figure 5). Different nucleotides at the center of the consensus sequence, that is, 'T' and 'C' on the A- and B-sites, respectively, might explain the preference for the B-site.

Yoo *et al.* have recently identified a circadian enhancer (E2) with a non-canonical 5'-CACGTT-3' E-box located 20 bp upstream of the *mPer2* transcription start site and demonstrated that a 210 bp promoter region with the E2 enhancer but without the B-site, is sufficient for *Per2* oscillation (24). Here, we performed real-time luciferase assays in NIH3T3 cells using the *mPer2* (−798 to +331) promoter containing the E2 enhancer as well as the novel E4BP4-binding site (B-site). Our findings showed that the novel *cis*-element for E4BP4 binding is required for robust circadian expression of *Per2* in the cell-autonomous core clock as well as the E2 enhancer, indicating that E4BP4 is a key negative regulator of the mammalian circadian clock.

The *Drosophila* circadian oscillator consists of interlocked *period/timeless* and *dClock* transcriptional/translational feedback loops (46–49). Within these loops, VRI negatively regulates *period* expression, which is activated by the dCLOCK:CYCLE complex (CYCLE is also known as dBMAL1), through the repression of *dClock* promoter activity (12,26,27). We showed that E4BP4, which is a mammalian homologue of *vri*, functions as a repressor of *Per2* transcription through the novel E4BP4-binding site (B-site) and that E4BP4 must bind to the B-site for the robust circadian expression of *Per2* in the cell-autonomous clock. These findings demonstrate the importance of negative

regulation by the direct binding of E4BP4 as well as of positive regulation by CLOCK:BMAL1 in the mammalian circadian clock. Taken together, VRI/E4BP4 seems to function as a negative factor of *Period* oscillation in the circadian clock of *Drosophila* and mammals.

Missense mutations in clock genes have recently been linked to familial advanced (50,51) and delayed (52) sleep phase syndromes, an abnormality in the circadian timing system that affects the timing of sleep. Here we show the importance of negative regulation by E4BP4 for the circadian expression of *Per2*. As with these clock components, the identification of a nucleotide polymorphism in *E4BP4* should bring new insight into sleep disorders.

SUPPLEMENTARY DATA

Supplementary Data are available at NAR Online.

ACKNOWLEDGEMENTS

The authors thank Dr Y. Nakajima for providing the plasmid containing *mPer2* promoter. We also thank Ms C. Iitaka, Dr K. Ohsaki and Mr Y. Hara for helpful discussion. This project was supported by operational subsidies from AIST (METI) and from the University of Tsukuba, and the Ministry of Education, Culture, Sports, Science and Technology. Funding to pay the Open Access publication charges for this article was provided by AIST (METI).

Conflict of interest statement. None declared.

REFERENCES

1. Dunlap,J.C. (1999) Molecular bases for circadian clocks. *Cell*, **96**, 271–290.
2. Kako,K. and Ishida,N. (1998) The role of transcription factors in circadian gene expression. *Neurosci. Res.*, **31**, 257–264.
3. Reppert,S.M. and Weaver,D.R. (2002) Coordination of circadian timing in mammals. *Nature*, **418**, 935–941.
4. Panda,S., Hogenesch,J.B. and Kay,S.A. (2002) Circadian rhythms from flies to human. *Nature*, **417**, 329–335.
5. Konopka,R.J. and Benzer,S. (1971) Clock mutants of *Drosophila melanogaster*. *Proc. Natl Acad. Sci. USA*, **68**, 2112–2116.
6. Bargiello,T.A., Jackson,F.R. and Young,M.W. (1984) Restoration of circadian behavioural rhythms by gene transfer in *Drosophila*. *Nature*, **312**, 752–754.
7. Reddy,P., Zehring,W.A., Wheeler,D.A., Pirrotta,V., Hadfield,C., Hall,J.C. and Rosbash,M. (1984) Molecular analysis of the *period* locus in *Drosophila melanogaster* and identification of a transcript involved in biological rhythms. *Cell*, **38**, 701–710.
8. Myers,M.P., Wager-Smith,K., Wesley,C.S., Young,M.W. and Sehgal,A. (1995) Positional cloning and sequence analysis of the *Drosophila* clock gene, *timeless*. *Science*, **270**, 805–808.
9. Allada,R., White,N.E., So,W.V., Hall,J.C. and Rosbash,M. (1998) A mutant *Drosophila* homolog of mammalian *Clock* disrupts circadian rhythms and transcription of *period* and *timeless*. *Cell*, **93**, 791–804.
10. Rutila,J.E., Suri,V., Le,M., So,W.V., Rosbash,M. and Hall,J.C. (1998) CYCLE is a second bHLH-PAS clock protein essential for circadian rhythmicity and transcription of *Drosophila period* and *timeless*. *Cell*, **93**, 805–814.
11. Price,J.L., Blau,J., Rothenfluh,A., Abodeely,M., Kloss,B. and Young,M.W. (1998) *double-time* is a novel *Drosophila* clock gene that regulates PERIOD protein accumulation. *Cell*, **94**, 83–95.
12. Blau,J. and Young,M.W. (1999) Cycling *willie* expression is required for a functional *Drosophila* clock. *Cell*, **99**, 661–671.

13. Tei,H., Okamura,H., Shigeyoshi,Y., Fukuhara,C., Ozawa,R., Hirose,M. and Sakaki,Y. (1997) Circadian oscillation of a mammalian homologue of the *Drosophila period* gene. *Nature*, **389**, 512–516.

14. Sun,Z.S., Albrecht,U., Zhuchenko,O., Bailey,J., Eichele,G. and Lee,C.C. (1997) *RIGUI*, a putative mammalian ortholog of the *Drosophila period* gene. *Cell*, **90**, 1003–1011.

15. Shearman,L.P., Zylka,M.J., Weaver,D.R., Kolakowski,L.F., Jr and Reppert,S.M. (1997) Two *period* homologs: circadian expression and photic regulation in the suprachiasmatic nuclei. *Neuron*, **19**, 1261–1269.

16. Albrecht,U., Sun,Z.S., Eichele,G. and Lee,C.C. (1997) A differential response of two putative mammalian circadian regulators, *mper1* and *mper2*, to light. *Cell*, **91**, 1055–1064.

17. Takumi,T., Matsubara,C., Shigeyoshi,Y., Taguchi,K., Yagita,K., Maebayashi,Y., Sakakida,Y., Okumura,K., Takashima,N. and Okamura,H. (1998) A new mammalian *period* gene predominantly expressed in the suprachiasmatic nucleus. *Genes Cells*, **3**, 167–176.

18. Takumi,T., Taguchi,K., Miyake,S., Sakakida,Y., Takashima,N., Matsubara,C., Maebayashi,Y., Okumura,K., Takekida,S., Yamamoto,S. *et al.* (1998) A light-independent oscillatory gene *mPer3* in mouse SCN and OVLT. *EMBO J.*, **17**, 4753–4759.

19. Sakanoto,K., Nagase,T., Fukui,H., Horikawa,K., Okada,T., Tanaka,H., Sato,K., Miyake,Y., Ohara,O., Kako,K. *et al.* (1998) Multitissue circadian expression of rat *period* homolog (*rPer2*) mRNA is governed by the mammalian circadian clock, the suprachiasmatic nucleus in the brain. *J. Biol. Chem.*, **273**, 27039–27042.

20. Zheng,B., Larkin,D.W., Albrecht,U., Sun,Z.S., Sage,M., Eichele,G., Lee,C.C. and Bradley,A. (1999) The *mPer2* gene encodes a functional component of the mammalian circadian clock. *Nature*, **400**, 169–173.

21. Bae,K., Jin,X., Maywood,E.S., Hastings,M.H., Reppert,S.M. and Weaver,D.R. (2001) Differential functions of *mPer1*, *mPer2*, and *mPer3* in the SCN circadian clock. *Neuron*, **30**, 525–536.

22. Zheng,B., Albrecht,U., Kaasik,K., Sage,M., Lu,W., Vaishnav,S., Li,Q., Sun,Z.S., Eichele,G., Bradley,A. *et al.* (2001) Nonredundant roles of the *mPer1* and *mPer2* genes in the mammalian circadian clock. *Cell*, **105**, 683–694.

23. Yamamoto,Y., Yagita,K. and Okamura,H. (2005) Role of cyclic *mPer2* expression in the mammalian cellular clock. *Mol. Cell. Biol.*, **25**, 1912–1921.

24. Yoo,S.H., Ko,C.H., Lowrey,P.L., Buhr,E.D., Song,E.J., Chang,S., Yoo,O.J., Yamazaki,S., Lee,C. and Takahashi,J.S. (2005) A noncanonical E-box enhancer drives mouse *Period2* circadian oscillations *in vivo*. *Proc. Natl Acad. Sci. USA*, **102**, 2608–2613.

25. Akashi,M., Ichise,T., Mamine,T. and Takumi,T. (2006) Molecular mechanism of cell-autonomous circadian gene expression of *Period2*, a crucial regulator of the mammalian circadian clock. *Mol. Biol. Cell*, **17**, 555–565.

26. Cyran,S.A., Buchsbaum,A.M., Reddy,K.L., Lin,M.C., Glossop,N.R., Hardin,P.E., Young,M.W., Storti,R.V. and Blau,J. (2003) *vrille*, *Pdp1*, and *dClock* form a second feedback loop in the *Drosophila* circadian clock. *Cell*, **112**, 329–341.

27. Glossop,N.R., Houl,J.H., Zheng,H., Ng,F.S., Dudek,S.M. and Hardin,P.E. (2003) *VRILLE* feeds back to control circadian transcription of *Clock* in the *Drosophila* circadian oscillator. *Neuron*, **37**, 249–261.

28. Doi,M., Nakajima,Y., Okano,T. and Fukada,Y. (2001) Light-induced phase-delay of the chicken pineal circadian clock is associated with the induction of *cE4bp4*, a potential transcriptional repressor of *cPer2* gene. *Proc. Natl Acad. Sci. USA*, **98**, 8089–8094.

29. Mitsui,S., Yamaguchi,S., Matsuo,T., Ishida,Y. and Okamura,H. (2001) Antagonistic role of E4BP4 and PAR proteins in the circadian oscillatory mechanism. *Genes Dev.*, **15**, 995–1006.

30. Ueda,H.R., Hayashi,S., Chen,W., Sano,M., Machida,M., Shigeyoshi,Y., Iino,M. and Hashimoto,S. (2005) System-level identification of transcriptional circuits underlying mammalian circadian clocks. *Nature Genet.*, **37**, 187–192.

31. Tojo,M., Matsuzaki,K., Minami,T., Honda,Y., Yasuda,H., Chiba,T., Sayo,H., Fujii-Kuriyama,Y. and Nakao,M. (2002) The aryl hydrocarbon receptor nuclear transporter is modulated by the SUMO-1 conjugation system. *J. Biol. Chem.*, **277**, 46576–46585.

32. Oishi,K., Amagai,N., Shirai,H., Kadota,K., Ohkura,N. and Ishida,N. (2005) Genome-wide expression analysis reveals 100 adrenal gland-dependent circadian genes in the mouse liver. *DNA Res.*, **12**, 191–202.

33. Ueda,H.R., Chen,W., Adachi,A., Wakamatsu,H., Hayashi,S., Takasugi,T., Nagano,M., Nakahama,K., Suzuki,Y., Sugano,S. *et al.* (2002) A transcription factor response element for gene expression during circadian night. *Nature*, **418**, 534–539.

34. Onishi,Y. and Kiyama,R. (2003) Interaction of NF-E2 in the human β -globin locus control region before chromatin remodeling. *J. Biol. Chem.*, **278**, 8163–8171.

35. Welsh,D.K., Logothetis,D.E., Meister,M. and Reppert,S.M. (1995) Individual neurons dissociated from rat suprachiasmatic nucleus express independently phased circadian firing rhythms. *Neuron*, **14**, 697–706.

36. Nagoshi,E., Saini,C., Bauer,C., Larocque,T., Naef,F. and Schibler,U. (2004) Circadian gene expression in individual fibroblasts: cell-autonomous and self-sustained oscillators pass time to daughter cells. *Cell*, **119**, 693–705.

37. Yamazaki,S., Numano,R., Abe,M., Hida,A., Takahashi,R., Ueda,M., Block,G.D., Sakaki,Y., Menaker,M. and Tei,H. (2000) Resetting central and peripheral circadian oscillators in transgenic rats. *Science*, **288**, 682–685.

38. Yoo,S.H., Yamazaki,S., Lowrey,P.L., Shimomura,K., Ko,C.H., Buhr,E.D., Siepka,S.M., Hong,H.K., Oh,W.J., Yoo,O.J. *et al.* (2004) *PERIOD2::LUCIFERASE* real-time reporting of circadian dynamics reveals persistent circadian oscillations in mouse peripheral tissues. *Proc. Natl Acad. Sci. USA*, **101**, 5339–5346.

39. Balsalobre,A., Damiola,F. and Schibler,U. (1998) A serum shock induces circadian gene expression in mammalian tissue culture cells. *Cell*, **93**, 929–937.

40. Brandes,C., Plautz,J.D., Stanewsky,R., Jamison,C.F., Straume,M., Wood,K.V., Kay,S.A. and Hall,J.C. (1996) Novel features of *drosophila period* transcription revealed by real-time luciferase reporting. *Neuron*, **16**, 687–692.

41. Balsalobre,A., Marcacci,L. and Schibler,U. (2000) Multiple signaling pathways elicit circadian gene expression in cultured Rat-1 fibroblasts. *Curr. Biol.*, **10**, 1291–1294.

42. Cowell,I.G., Skinner,A. and Hurst,H.C. (1992) Transcriptional repression by a novel member of the bZIP family of transcription factors. *Mol. Cell Biol.*, **12**, 3070–3077.

43. Hough,C., Cuthbert,C.D., Notley,C., Brown,C., Hegadorn,C., Berber,E. and Lillicrap,D. (2005) Cell type-specific regulation of von Willebrand factor expression by the *E4BP4* transcriptional repressor. *Blood*, **105**, 1531–1539.

44. Balsalobre,A., Brown,S.A., Marcacci,L., Tronche,F., Kellendonk,C., Reichardt,H.M., Schutz,G. and Schibler,U. (2000) Resetting of circadian time in peripheral tissues by glucocorticoid signaling. *Science*, **289**, 2344–2347.

45. Lai,C.K. and Ting,L.P. (1999) Transcriptional repression of human hepatitis B virus genes by a bZIP family member, E4BP4. *J. Virol.*, **73**, 3197–3209.

46. Allada,R., Emery,P., Takahashi,J.S. and Rosbash,M. (2001) Stopping time: the genetics of fly and mouse circadian clocks. *Annu. Rev. Neurosci.*, **24**, 1091–1119.

47. Hall,J.C. (2005) Systems approaches to biological rhythms in *Drosophila*. *Methods Enzymol.*, **393**, 61–185.

48. Stanewsky,R. (2003) Genetic analysis of the circadian system in *Drosophila melanogaster* and mammals. *J. Neurobiol.*, **54**, 111–147.

49. Young,M.W. and Kay,S.A. (2001) Time zones: a comparative genetics of circadian clocks. *Nature Rev. Genet.*, **2**, 702–715.

50. Toh,K.L., Jones,C.R., He,Y., Eide,E.J., Hinz,W.A., Virshup,D.M., Ptacek,L.J. and Fu,Y.H. (2001) An *hPer2* phosphorylation site mutation in familial advanced sleep phase syndrome. *Science*, **291**, 1040–1043.

51. Xu,Y., Padiath,Q.S., Shapiro,R.E., Jones,C.R., Wu,S.C., Saigoh,N., Saigoh,K., Ptacek,L.J. and Fu,Y.H. (2005) Functional consequences of a *CK1 δ* mutation causing familial advanced sleep phase syndrome. *Nature*, **434**, 640–644.

52. Ebisawa,T., Uchiyama,M., Kajimura,N., Mishima,K., Kamei,Y., Katoh,M., Watanabe,T., Sekimoto,M., Shibui,K., Kim,K. *et al.* (2001) Association of structural polymorphisms in the human *period3* gene with delayed sleep phase syndrome. *EMBO Rep.*, **2**, 342–346.



6 Review article

7 Circadian clock, cancer and lipid metabolism

8 Norio Ishida ^{a,b,*}

9 ^a Clock Cell Biology, Department of Biological Resources and Functions,
10 National Institute of Advanced Industrial Science and Technology (AIST), 6-5 Tsukuba Center,
11 1-1 Higashi, Tsukuba 305-8566, Japan

12 ^b Graduate School of Life and Environmental Sciences, University of Tsukuba, Tsukuba, Ibaraki 305-8502, Japan

13 Received 25 October 2006; accepted 25 December 2006

14 Abstract

15 Genetic analysis has revealed that mammalian circadian oscillator is driven by a cell autonomous transcription/translation-based negative
16 feedback loop, wherein positive elements (CLOCK and BMAL1) induce the expression of negative regulators (Periods, CRY1 and CRY2) that
17 inhibit the transactivation of positive regulators. Recent research reveals that this clock feedback loop affects many aspects of our physiology, such
18 as cell cycle and lipid metabolism. In this review, I summarize the molecular links between the circadian clock mechanism and the cell cycle, and
19 between the clock and lipid metabolism. Recent studies of clock mutants also suggest that clock molecules play a role as stress sensors. Lastly, we
20 propose the importance of sterol for entraining peripheral clocks.

21 © 2007 Elsevier Ireland Ltd and the Japan Neuroscience Society. All rights reserved.

22 **Keywords:** Circadian; Lipid; Cancer

23 Contents

1. Introduction	000
1.1. Coupling of the circadian clock and the cell cycle	000
1.2. Timeless couple circadian with cell cycle	000
1.3. Light affect circadian clock and cell cycle gene expression	000
1.4. Circadian clock genes and Cancer: a role of clock genes for environmental stress sensors	000
1.5. Cancer and clock genes—the unusual rhythmic expression of growth factor genes	000
1.6. Mouse clock mutants and obesity	000
1.7. The circadian clock and cholesterol metabolism	000
1.8. Circadian clock and torpor-change of lipid metabolism at hibernation	000
Acknowledgements	000
References	000

38 **1. Introduction**

39 The behavior and physiology of most organisms are
40 subject to circadian, 24-h rhythmicity. Circadian oscillators
41 are controlled by negative feedback loops in clock gene

42 expression from bacteria to mammals. CLOCK forms
43 heterodimers with another bHLH-PAS transcription factor,
44 BMAL1, and transactivates other clock genes such as *period1*
45 (*Per1*), *Per2*, *cryptochromel* (*Cry1*) and *Cry2* via E-box
46 elements in their promoters (Dunlap, 1999; Ishida et al.,
47 1999; Schibler and Sassone-corsi, 2002; Ishida et al., 2001).
48 At least nine clock genes (*clock*, *per1* and 2, *Bmal1*, *cry1* and
49 2, *Tim*, *casein kinase1* and *glycogen synthase kinase 3b*)
50 generate circadian rhythms in mammals, where most of these
51 genes were identified as homologues from *Drosophila* clock
52 genes except for *Clock* (Table 1). Molecules generally of
53

* Correspondence address: Clock Cell Biology, Department of Biological Resources and Functions, National Institute of Advanced Industrial Science and Technology (AIST), 6-5 Tsukuba Center, 1-1 Higashi, Tsukuba 305-8566, Japan. Fax: +81 29 861 9499.

E-mail address: n.ishida@aist.go.jp.

Table 1

A list of clock genes in *Drosophila* and mammals

<i>Drosophila</i>	Mouse
Period	mPeriod1 mPeriod2 mPeriod3
Timeless	ND
Timeout/timeless2	mTimeless
Cryptochrome	mCryptochrome1 mCryptochrome2
Clock(Jrk)	Clock NPAS2/MOP4
Cycle	Bmal1/MOP3 Bmal2/MOP9/CLIF
Doubletime	Casein kinase 1 epsilon Casein kinase 1 delta
Shaggy	GSK3β
Protein phosphatase 2A	Protein phosphatase 2A
Slimb	FWD1 (?)
Vrille	E4BP4

Most clock genes in mammals are identified from homologue to *Drosophila* clock genes except for mouse *Clock* gene. *Drosophila cry* have a role for input pathway in circadian rhythm. ND; not determined for real orthologue.

53

transcription factors that oscillate over a 24-h period control
54 their own expression in a circadian fashion seem critical to
55 the generation of circadian rhythm of most organisms
56 (Dunlap, 1999; Ishida et al., 1999). However, some kinases
57 that are involved in protein degradation (casein kinase 1) and
58 nuclear translocation (glycogen synthase kinase 3b) are also
59 important for defining the concentration of clock molecules at
60 specific subcellular sites (Ishida et al., 2001; Iitaka et al.,
61 2005).

62 The suprachiasmatic nucleus (SCN) of the anterior
63 hypothalamus in mammals is the central oscillator that
64 controls approximately 24-h periodicity (circadian rhythms)
65 in behavior and physiology (Schibler and Sassone-corsi,
66 2002). Neurons in the SCN receive light information via the
67 retinohypothalamic tract and the phase of the circadian clock
68 adapts to photoperiods (Hastings, 1997). Other peripheral
69 tissues are also equipped with endogenous oscillators using
70 clock gene products. In general, the expression of mRNA and
71 proteins of mammalian clock genes including those involved in
72 phosphorylation in the SCN and in other peripheral tissues
73 oscillates in a robust circadian manner (Dunlap, 1999; Ishida
74 et al., 1999; Schibler and Sassone-corsi, 2002) Thus, the
75 oscillation of such clock genes is a useful marker for
76 determining the phase and period of peripheral clocks and
77 the central clock (Oishi et al., 2002; Sakamoto et al., 1998).
78 Only recently the importance of circadian system has become
79 apparent for the regulation of the cell cycle and metabolism
80 because of a convergence of data from microarray analysis
81 using clock mutants and clock gene expression as a marker. I
82 will propose a role of clock gene products for stress sensor
83 considering recent progress of many physiological phenomena
84 from circadian clock.

1.1. Coupling of the circadian clock and the cell cycle

86 Circadian clock and cell cycles are global regulatory
87 systems found in almost all organisms. Similarly, the both of
88 cycles are periodic for ca. 24 h, and intrinsic to most cells.
89 Circadian cycles of clock gene expression persists in every cell,
90 in contrast the cell cycles where consists of Gap1 (G1), DNA
91 synthesis (S), Gap2 (G2), and mitosis (M) phases are stopped at
92 G1 or G0, which need a specific trigger to start such as liver
93 regeneration (Nyberg et al., 2002). It is clear, further, that in
94 mammals the circadian clock does not depend on cell cycle
95 because adult neuronal cells do not divide yet, they exhibit
96 robust circadian rhythm of gene expression. When cell division
97 is inhibited, rhythmic clock gene expression continue (Nagoshi
98 et al., 2004).

99 Although circadian and cell cycles consist of distinct
100 molecular mechanisms, a recent review suggests that these
101 cycles are linked in mammals (Lowrey and Takahashi, 2004).
102 Surprisingly, recent two papers implicate the circadian clock in
103 the regulation of cell division cycles because expression of key
104 cell cycle regulators is altered by circadian clock mutations in
105 mammals (Oishi et al., 2003; Matsuo et al., 2003). Matsuo et al.
106 (2003) showed that liver regeneration is impaired in cry-
107 deficient mice and that the expression profiles of cyclin B1,
108 CDC2, cyclin D1 and wee1 differ from those of wild-type mice.
109 The G2/M transition is a crucial point for the cell cycle which is
110 controlled by the Cdc2 kinase/cyclin B complex. Another cell
111 cycle regulator from G2 to M is WEE1. Matsuo et al. concluded
112 that the negative feedback loop of circadian clock genes can
113 initiate the cell cycle in the regenerating liver by regulating
114 wee1 gene expression through a direct binding of CLOCK/
115 Bmal1 to E-box in the promotor of wee1 gene. Oishi et al.
116 (2003) also showed using Affymetrix DNA microarray analysis
117 that hepatic wee1 mRNA is damped in Clock mutant mice
118 whereas mRNA expression remains continuously high in cry-
119 deficient mice. These data indicated that wee1 mRNA
120 expression can be achieved by CLOCK/BMAL1 binding or
121 repressed by CRY at E-boxes even in vivo. This microarray
122 study also demonstrated damped circadian expression of
123 growth-arrest and DNA damage-inducible (GADD) 45a and
124 GADD45b mRNAs in clock mutant mice, but high levels of
125 these mRNAs in cry-deficient mice (Oishi et al., 2003). The
126 main role of GADDs is to block cell cycle at G1 and G2
127 checkpoints in response to DNA damage. The GADD genes are
128 up-regulated in response to a variety of stressors including
129 γ -radiation. In response to DNA-damage inducers including
130 UV radiation, γ -radiation, and the alkylating agent methyl
131 methanesulfonate (MMS), mammalian cells can prevent cell
132 cycle progression by controlling critical regulators, the GADD
133 genes. Furthermore, Fu et al. (2002) showed that Cyclin D1 and
134 Gadd45a, both of which are themselves targets of c-myc
135 activation, oscillate in wild type, but exhibit altered circadian
136 rhythm in Per2 mutant mice. Thus, the cyclic expression of
137 GADD45a and GADD45b suggests that peripheral clocks may
138 control the checkpoint of cell cycle in the mouse liver. Taken
139 together, G2/M transition is a target for the gating of circadian
140 clock.

141 1.2. *Timeless couple circadian with cell cycle*

142
143 The *Timeless* gene in *Drosophila* is necessary for the
144 generation of circadian rhythms. Although we (Sakamoto et al.,
145 2000) and others (Koike et al., 1998; Sangoram et al., 1998)
146 have identified mammalian *Timeless* (*Tim*) by searching the
147 dPERIOD-PAS binding protein from rat brain (the former) or in
148 silico cloning using dTim homology (the latter), the role
149 of *TIMELESS* protein has remained obscure because Tim
150 knockout is lethal to embryos (Lowrey and Takahashi, 2004).
151 However, Barnes et al. (2003) reported that the down-regulation
152 of full-length mammalian Tim in SCN slices reduces the firing
153 activity of the SCN and affects the expression levels of Per1,
154 Per2, Per3, Cry1 and Cry2. Thus, mammalian Tim might
155 function in the generation of circadian rhythms in the SCN.
156 However, mammalian Tim has higher sequence similarity with
157 drosophila(d)Tim2/dTimeout, which does not function for
158 circadian clock. Studies in *Drosophila* have shown that high
159 levels of dTim2 are expressed at larval stages (Benna et al.,
160 2000). In mammals, mouse Tim appear to function in branching
161 of the embryonic kidneys and lungs because of malformation of
162 these organs in knock out mice, suggesting a developmental
163 role of mTim (Li et al., 2000). Mammalian Tim has structural
164 similarity to many cell-cycle related proteins from other
165 species: budding yeast Tof1 (Park and Sternblanz, 1999) fission
166 yeast DNA damage check points protein Swi1 (Noguchi et al.,
167 2003) and *C. elegans* chromosome cohesion protein TIM-1
168 (Chan et al., 2003). A recent report by Sancar's group indicates
169 that mammalian Tim is also involved in cell cycle-replication
170 and intra-s check points (Keziban et al., 2005). They found that
171 hTim expression is cell cycle regulated and that hTim binds to
172 the checkpoint proteins Chk1 and ATR-ATRIP complex in a
173 hydroxyurea damage-dependent manner. Furthermore, Tim
174 siRNA application causes entry into mitosis before DNA
175 replication is completed in Hela cells and increases hydroxyurea-induced
176 premature chromatin condensation. These data indicate that Tim plays a role in the regulation of the
177 mammalian cell cycle. Moreover, hTim binds to mCry2 and the
178 down-regulation of Per2 protein by Tim knock-down through
179 its siRNA application in HEK293T cells suggests that hTim
180 plays a role for the circadian clock. If this is the case,
181 mammalian Tim protein seems to be a missing link protein
182 coupling cell cycle and circadian cycle.
183

184 1.3. *Light affect circadian clock and cell cycle gene 185 expression*

186 A common feature of clock and cell cycles is their sensing to
187 light. Effect of light appeared to be very important for
188 considering of cell cycle and circadian cycle. Light directly
189 regulates circadian rhythmicity in most zebrafish tissues,
190 because autonomous clocks in cultured cells and tissues have
191 the ability to entrain to light. Hirayama et al. reported that light
192 induces the expression of zebrafish(z)Wee1, which is involved
193 in G2/M transition and the circadian clock genes, zCry1a and
194 zPer2 (Hirayama et al., 2005). They found that the importance
195 of light induced Fos binding to AP-1 sites in promoters of

196 zWee1 and zCry1a genes through chromatin remodeling of
197 histone H3. In zebrafish, light seems to be very important to
198 connect cell cycle players and clock players by inducing FOS.
199 In mammals, AP-1 transiently inhibits G2/M progression
200 through stimulation of Wee1 via an AP-1 element in its
201 promoter (Kawasaki et al., 2003; Russell and Nurse, 1987). As
202 noted above, Wee1 expression in the mouse liver is also
203 dependent on CLOCK/BMAL1 transactivation through an E-
204 box (Oishi et al., 2003; Matsuo et al., 2003). The similarity
205 indicates that lights effect is quit old system. Even in the
206 flagellate alga *Euglena*, the progression of G2/M is induced by
207 light and its circadian control might be an integral part of the
208 cell division cycle (Hagiwara et al., 2002). From an
209 evolutionary viewpoint, light-induced change of players in
210 both of clock and cell cycles might suggest that the missing
211 molecules of cell and circadian cycle coupling may be a sensor
212 for light. It is clear that these findings between divergent species
213 bring new insights into the evolution of circadian and cell
214 cycles.

215 1.4. *Circadian clock genes and Cancer: a role of clock 216 genes for environmental stress sensors*

217 Although many clinical physicians noticed that chronotherapy
218 is useful for the timing of application for anti-cancer drugs,
219 the molecular mechanism underlying this phenomena is not
220 understand. Surprisingly, recent studies have indicated a role of
221 clock gene products as negative regulators for the generation of
222 cancer. The incidence of radiation-induced lymphoma in Per2
223 mutant mice is increased and irradiated Per2 mutants die early
224 (Fu et al., 2002). These results were explained by increased c-
225 Myc expression and decreased p53 expression in mice with a
226 Per2 loss-of-function mutation. They also showed that per2
227 mutants show increased sensitivity to γ -radiation and tumour
228 development. Furthermore, they indicated that increased radio
229 sensitivity in per2 mutants due to a role of clock genes for early
230 responsive genes to γ -radiation, because the dysregulated
231 mRNA induction of clock, cry1 and cry2 was detected in per2
232 mutant mice. A potential role of Per2 in this lymphoma seems
233 to be as a gamma irradiation-responsive gene.

234 The notion that clock genes function as stress sensing factors
235 is plausible, since sleep deprivation in *Drosophila* (Shaw et al.,
236 2002) and food deprivation in mice (Kobayashi et al., 2004)
237 alter the expression of circadian clock genes. In *Drosophila*,
238 sleep deprivation in *clock* mutants have been shown to cause an
239 early death that can be avoided by preheating the flies via the
240 induction of heat-shock proteins (Shaw et al., 2002). Depriving
241 mice of food for three days reduces peak levels of Per2 and DBP
242 mRNA expression in the liver and heart and significantly
243 induces Per1 expression in these tissues (Kobayashi et al.,
244 2004). Another report indicated that CLOCK/BMAL1 activity
245 modulates the effects of genotoxic stress such as cyclophosphamide-induced
246 toxicity through altering B cell responses (Gorbacheva et al., 2005). Taken together, these studies suggest
247 that clock genes play roles in stress sensing and releasing.

248 The circadian system is thought to have evolved as an
249 adaptation to daily changes in the environmental such as light,
250

250
251 temperature, food and toxic factors. When stress such as γ
252 irradiation or sleep deprivation fails to inform the circadian
253 clock in mouse Per2 mutants or *Drosophila* clock mutants,
254 tumors form and death occur at early ontogeny. Thus, circadian
255 clock gene products have a role as environmental stress sensors.

256 *1.5. Cancer and clock genes—the unusual rhythmic
257 expression of growth factor genes*

258 Surprisingly, recent two papers reported that the unusual
259 rhythmic expression of growth factor genes were observed in
260 implanted tumors in mice. Koyanagi et al. (2003) reported that
261 vascular endothelial growth factors (VEGF) in implanted
262 sarcoma cells are expressed in an unusual high amplitude of
263 circadian manner, in contrast, no significant rhythmic expression
264 of VEGF was detected in normal tissues. Furthermore, the
265 rhythmic expression of VEGF in Sarcoma 180 cells has been
266 positively regulated mainly through the hypoxia-inducible
267 factor, HIF-1 α , binding to its promoter, and negatively, through
268 PER2-HIF-1 α binding during different circadian time in mice.
269 This also showed a role of PER2 for suppression of tumor
270 generation (Fu et al., 2002) through the down regulation of
271 VEGF gene expression. This is the first study to show that
272 tumor cells use the unusual high amplitude of circadian
273 expression of growth factors as a strategy for growing tumors.
274 The same group also found that the circadian rhythms of the
275 protein and mRNA for methionine aminopeptidase 2, which is
276 involved in the growth of endothelial cells during tumor
277 angiogenesis, are also unusually rhythmic with high amplitude
278 in implanted tumor cells (Nakagawa et al., 2004). Their data
279 suggested that the 24-h rhythm of methionine aminopeptidase 2
280 activity is regulated by the transcription factors of clock gene
281 products, CLOCK/BMAL1 in the positive limb of clock
282 feedback loop. If this is indeed a strategy through which tumor
283 cells can grow in a normal environment, then it can be applied
284 to the timing of anti-tumor drugs to minimize side-effects and
285 increase drug efficacy as shown by Ohdo group (Koyanagi
286 et al., 2003).

287 Another group showed different data that the daily ordering
288 of tumor cell clock gene expression might not be correlated to
289 the daily gating of DNA synthesis by breast cancer cells,
290 because cyclin E protein peaks 2 times each day, whereas the
291 Bmal1 gene peaks once a day in cancer cells (You et al., 2005)
292 This group did not find any significant daily rhythms associated
293 with mPer1 and mPer2 gene expression in transplanted
294 syngeneic mammary tumor cells. Mammary epithelial cells
295 might be a different mechanism with sarcoma. But, in vitro,
296 per2-luciferase real-time reporter assay demonstrate the rhythm
297 of clock genes appeared circadian after dexamethasone
298 stimulation in Sarcoma 180 (sarcoma) cells as well as NIH3T3
299 cells (Ohno, T., Onishi, Y., Hara, Y., Ishida, N., unpublished
300 data). The data indicate that the circadian clock is still working
301 even in sarcoma cells.

302 Taken together, the coupling between circadian clock genes
303 and cancer appeared to be depending on specific developing
304 times in various tumor tissues *in vivo*. In our hands, clock
305 mutations seem to affect the susceptibility of normal cells to

306 become tumors because the lack of stress sensing and stress
307 releasing in clock mutants might cause altered response to cell
308 immunity (Oishi et al., 2006c). The elucidation of this
309 connection between the feedback loop of circadian clock
310 genes and abnormal cell cycles in cancer should bring new
311 insights into the mechanisms of cancer and the strategies for its
312 treatment and prevention as well as the development of novel
313 anti-tumor drugs.

314 *1.6. Mouse clock mutants and obesity*

315 One new area of investigation in chronobiology is the
316 relationship between obesity and clock mutation. Clock mutant
317 mice had the Clock allele originally on a BALB/c and C57BL/6J
318 background (Vitaterna et al., 1994). The circadian periods of
319 drinking behavior of homozygous Clock mutant mice on a
320 BALB/c and C57BL/6J background were abnormally long,
321 eventually becoming arrhythmic in constant darkness. A
322 breeding colony was established by further backcrossing to
323 ICR mice, and the new congenic strain was subsequently
324 maintained by interbreeding for 10 generations. Interestingly,
325 *clock* on ICR mice exerted a longer phenotype (28 h period) of
326 behavior and body temperature with different periods in males
327 and females (Oishi et al., 2002; Ochi et al., 2003). Thus, the
328 background strain of *Clock* mutants affects behavioral
329 phenotypes (Vitaterna et al., 1994; Oishi et al., 2002).

330 Turek's group reported that *Clock* mutants on a BALB/c and
331 C57BL/6J become obese after 6 weeks of age even after being
332 fed with regular chow (Turek et al., 2005). Furthermore, they
333 showed that appetite regulating peptides, orexin and ghrelin as
334 well as cocaine- and amphetamine-regulated transcript (CART)
335 mRNA in the mediobasal hypothalamus of the brains of *clock*
336 mutant mice. This finding could explain why the mutant mice
337 have such a large appetite during day and night. However, some
338 questions unanswered in this report. Firstly, orexin and ghrelin
339 play roles in the induction of feeding, whereas CART reduces
340 feeding when centrally administered. Secondly, they showed
341 that serum leptin levels increase during the light phase in *Clock*
342 mutants, and leptin inhibits food intake. However, the authors
343 showed that food intake in *Clock* mutants is increased during
344 the light phase (resting time for nocturnal animals) and
345 suggested that this phenotype is one explanation for obesity.
346 Although their data could not explain how obesity and a
347 metabolic syndrome develop in *Clock* mutant mice, the notion
348 is very important because several genome-wide analyses have
349 already shown that lipid metabolism is altered in circadian
350 clock mutant mice (Schibler and Sassone-corsi, 2002; Lowrey
351 et al., 2004; Oishi et al., 2003, 2005a,b).

352 In contrast to results in BALB/c and C57BL/6J mice, Oishi
353 et al. (2006a) found that *clock* mutant mice with ICR
354 background and their sibling controls weigh the same when
355 fed with a normal diet. Furthermore, this ICR *clock* mutants on
356 a high-fat diet do not gain weight like their sibling controls and
357 orally administered fatty acids are not absorbed from the
358 intestines of *clock* mutants. These investigators also reported
359 that reduced levels of the cholecystokinin-A receptor and of
360 lipase in the pancreas disrupt fat absorption and thus reduced

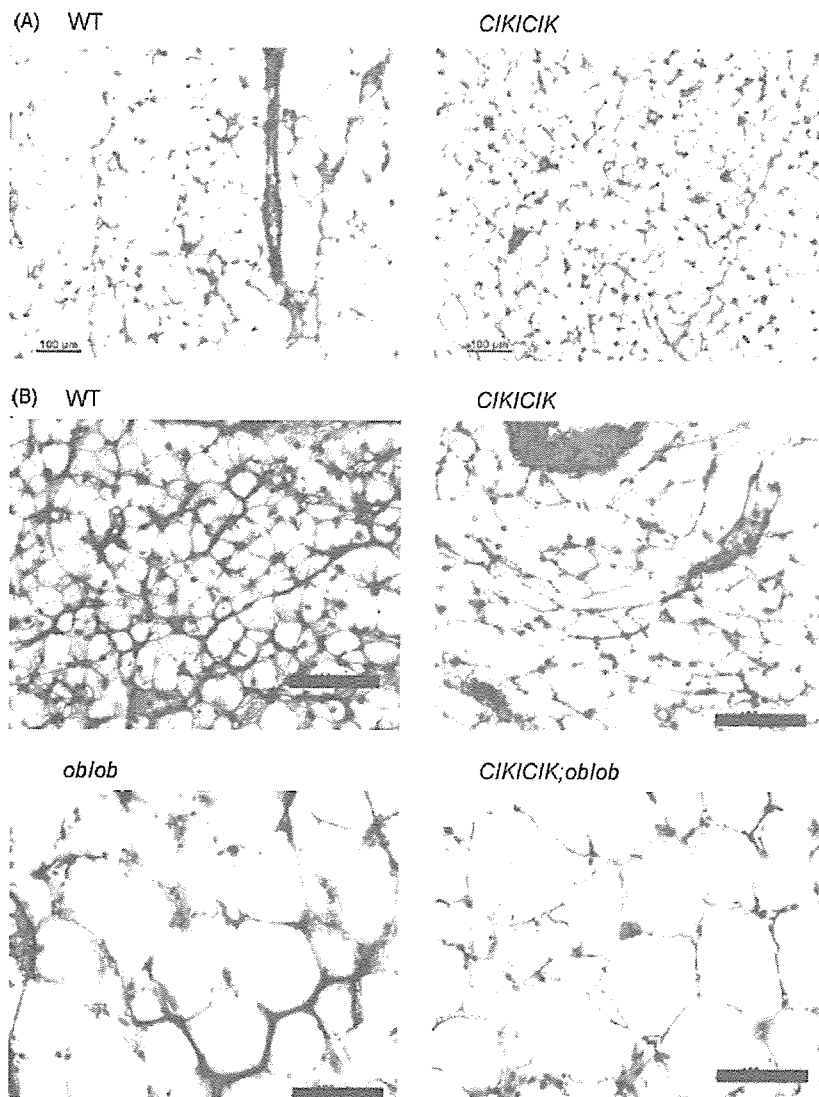


Fig. 1. (A) Cell size in adipose tissue of *Clock* mutant on Jcl mice is smaller than that of the sibling control. Epididymal adipose tissues from male wild-type (WT), homozygous *Clock* mutant (*Clk/Clk*) on Jcl. (B) Enlargement of cell size in adipose tissue of *Clock* mutated leptin-deficient *ob/ob* mice. Epididymal adipose tissues from male wild-type (WT), homozygous *Clock* mutant (*Clk/Clk*), leptin-deficient (*ob/ob*), and *Clk/Clk;ob/ob* mice were stained with hematoxylin and eosin. All four genotypes comes from the brothers after crossing *Clock* mutants on Jcl with *ob/ob* on C57/BL6. Bars indicate 100 μ m.

360 weight induced by a high-fat diet in the ICR *Clock* mutant mice.
361 One reason for the apparently contradictory effect of the clock
362 gene on obesity might be the background of the clock mutants;
363 the former were C57/BL6 (long and arrhythmic behavior after
364 constant dark), whereas the latter were ICR (long phenotype,
365 28 h; Vitaterna et al., 1994; Oishi et al., 2002; Ochi et al., 2003).
366 Recent data of the latter ICR *Clock* mutants crossed with *ob/ob*
367 mice on C57/BL6 indicated the importance of background.
368 Interestingly, this clock mutated *ob/ob* mice with mixed
369 backgrounds showed gain weight, high triglycerol and high
370 cholesterol to wild in contrast to the slender phenotype of *Clock*
371 mutants on ICR (Oishi et al., 2006b,a). Furthermore, this clock
372 mutated *ob/ob* mice showed a phenotype of adipocyte
373 hypertrophy adding to *ob/ob* mice, but the ICR *Clock* mutants
374 showed hypotrophy (Fig. 1). Taken together, these data indicate
375

376 that normal CLOCK protein are required for the maintenance of
377 homeostatic balance of lipid metabolism.

1.7. The circadian clock and cholesterol metabolism

378 The circadian peak of blood glucocorticoids is controlled by
379 the SCN via the paraventricular nucleus (PVN) of the
380 hypothalamus, where neurons containing corticotropin-releas-
381 ing hormone (CRH) regulate the secretion of adrenocortico-
382 tropic hormone (ACTH) from the pituitary (Buijs et al., 2003).
383 This pathway is called the hypothalamic–pituitary–adrenal
384 (HPA) axis. A recent study has revealed that light induces gene
385 expression in the adrenal gland via the SCN-sympathetic
386 nervous system (Ishida et al., 2005). Glucocorticoid signaling is
387 thought to be an important time cue for peripheral clocks via
388

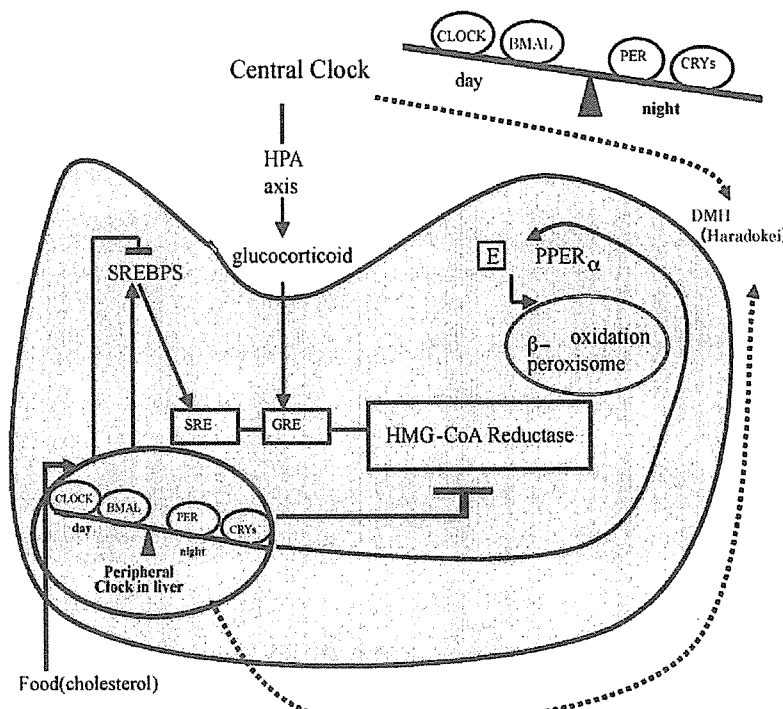


Fig. 2. Model of circadian sterol metabolism in peripheral clocks. Dietary cholesterol inhibit the expression of SREBPs and HMG-CoA reductase through a sterol sensing domain. The clock feedback loop regulate rhythmic PPAR α expression through E-boy. SRE; sterol response element, GRE; glucocorticoid response element. DMH; Dorsomedial hypothalamic nucleus. Dashed line means hypothetical. "Haradokei" in Japanese means the phenomena that we can tell about time when we feel hungry without watch. My hypothesis is that peripheral clock can feed back the information to the brain-site like DMH (so-called Haradokei) when food is available.

388 humoral pathway, the HPA axis or via neuronal pathway,
389 sympathetic nerves from the SCN (Balsalobre et al., 2000).

390 The key enzyme in the cholesterol biosynthetic pathway is
391 3-hydroxy-3 methylglutaryl-Coenzyme A (HMG-CoA) reductase, and daily variations in its hepatic activity have been
392 recognized since 1969 (Hamprecht et al., 1969). However, the
393 molecular mechanism of circadian mRNA of HMG-CoA
394 regulation has remained unknown until recently. A DNA
395 microarray study has shown that the adrenal gland is involved
396 in the circadian regulation of HMG-CoA reductase mRNA
397 expression in the mouse liver (Oishi et al., 2005a). Low levels
398 of dietary cholesterol significantly induce HMG-CoA reductase
399 mRNA in the rat liver and adrenal glands (food entrainable
400 peripheral clocks; Jurevics et al., 2000). Such induction
401 might be regulated by the selective binding of sterol regu-
402 latory element-binding protein family of transcription factors
403 (SREBPs) to SRE elements or E-boxes in vivo by sensing
404 dietary cholesterol levels. The SREBPs also regulate acetyl-
405 CoA carboxylase, fatty acid synthase and squalene synthase,
406 suggesting roles for SREBPs in cholesterol synthesis as well as
407 fatty acid metabolism (Patel et al., 2001). A sterol-sensing
408 domain in SREBPs is a candidate molecule in the pathway for
409 food-entrainable peripheral clock (Schibler et al., 2003),
410 because HMG-CoA reductase expression does not increase
411 in peroxisome proliferator-activated receptor- α (PPAR α)-null
412 mice during feeding (Patel et al., 2001). Exposing mice that
413 are usually nocturnal feeders to restricted feeding during the
414 day shifts the peak of SREBP-1 activation and HMG-CoA
415

416 reductase expression in the liver (Schibler et al., 2003). These
417 data suggest that cholesterol in food might be a role for
418 entraining peripheral clocks (Fig. 2). Restricted feeding does
419 not affect the central clock SCN (Schibler et al., 2003), but ad
420 libitum feeding during a light:dark reversal protocol seems to
421 be shift the putative central clock more effectively than fasting
422 because behavior reversed effectively (Kobayashi et al., 2004).
423 In the restricted feeding, the central clock which affect behavior
424 might be another site from the SCN, one possible site is
425 dorsomedial hypothalamic nucleus (DMH) which is considered
426 for monitoring food availability (Gooley et al., 2006). Since
427 daily variations in fatty acid synthase and HMG-CoA reductase
428 gene expression are attenuated or abolished in PPAR α -null mice
429 (Patel et al., 2001), PPAR α seems to play an important role in the
430 food entrainable expression of these sterol-regulated genes.
431 Interestingly, a recent report demonstrated that the circadian
432 clock gene product CLOCK is involved in the circadian
433 expression of PPAR α in mice (Oishi et al., 2005b). The molecular
434 mechanism of the transcriptional regulation of HMG-CoA
435 reductase by glucocorticoids will bring new insights into sterol
436 metabolism and clock molecules. Preliminary data from my
437 laboratory indicate that several GRE sites in HMG-CoA
438 reductase gene are important for glucocorticoid induction in
439 liver cells (Kohata, K., Shirai, H., Oishi, K., Ishida, N., in
440 preparation). Fig. 2 summarizes the pathways of HMG-CoA
441 reductase gene expression mentioned above. The expression of
442 HMG-CoA reductase gene are regulated by peripheral clock as
443 well as central clock.

444
445 1.8. Circadian clock and torpor-change of lipid
446 metabolism at hibernation

447 The tumor suppressor gene product, patched1, has a sterol-
448 sensing domain like HMG-CoA reductase (Borjigin et al.,
449 1999). Patched1 is the mammalian homologue of the
450 *Drosophila hedgehog* receptor and its transcription is strictly
451 regulated in a circadian manner in rat pineal gland. Sterol
452 metabolism in the pineal clock might be an interesting field
453 because this neuroendocrine gland plays an important role in
454 the regulation of seasonal clocks that might correlate with
455 annual lipid cycles in hibernators (Dark, 2005).

456 A recent breakthrough with torpor and hibernation field
457 by Dr. C.C. Lee's group is that constant darkness like
458 hibernation condition induced 5'-AMP and increased fat
459 catabolic enzyme procolipase in murine blood but not
460 increased in light-dark (LD) cycle condition. Under constant
461 dark for mice, 5'-AMP induced procolipase and torpor. These
462 data suggests that procolipase may have a role for the
463 maintenance of circadian state of brain for hibernation
464 (Zhang et al., 2006). As procolipase induction is disrupted
465 in per1/per2 double mutant mice, this is the first report to
466 link between molecular clock and torpor at substantial
467 level in mammals. The change of mammalian energy source
468 from sugars to lipids during torpor by enterostatin is an old
469 system as well as circadian system. Further study should
470 clarify a role of clock genes for the hibernation and lipid
471 catabolism.

472
473 Uncited reference

Miyazaki et al. (2004).

474 Acknowledgements

475 I appreciate Dr. Paul Hardin (Texas A&M) for proofreading
476 and critical comments of this manuscript. I also thanks Drs.
477 Cheng Chi Lee (University of Texas), G.T.J. van der Horst
478 (Erasmus Medical Center), Toru Takumi (Osaka Bioscience),
479 Paolo Sassone-Corsi (University of California Irvine) Paul
480 Hardin (Texas A&M) for coming and sharing brand new data in
481 20th IUBMB International Congress of Biochemistry and
482 Molecular Biology and 11th FAOBO Congress in Tsukuba and
483 Kyoto.

484 References

Balsalobre, A., Brown, S.A., Marcacci, L., et al., 2000. Resetting of circadian
time in peripheral tissues by glucocorticoid signaling. *Science* 289, 2344–
2347.

Barnes, J.W., Tischkau, S.A., Barnes, J.A., Mitchell, J.W., Burgoon, P.W.,
Hickok, J.R., Gillette, M.U., 2003. Requirement of mammalian *Timeless* for
circadian rhythmicity. *Science* 302, 439–442.

Benna, C., Scannapieco, P., Piccin, A., Sandrelli, F., Zordan, M., Rosato, E.,
Kyriacou, C.P., Valle, G., Costa, R., 2000. A second *timeless* gene in
Drosophila shares greater sequence similarity with mammalian *tim*. *Curr.*
Biol. 10, R512–R513.

Borjigin, J., Deng, J., Wang, M.M., Li, X., Blackshaw, S., Snyder, S.H., 1999.
Circadian rhythm of *patched1* transcription in the pineal regulated
by adrenergic stimulation and cAMP. *J. Biol. Chem.* 274 (49), 35012–
35015.

Buijs, R.M., Van Eden, C.G., Goncharuk, V.D., Kalsbeek, A., 2003. The
biological clock tunes the organs of the body: timing by hormones and
the autonomic nervous system. *J. Endocrinol.* 177, 17–26.

Chan, R.C., Chan, A., Jeon, M., Wu, T.F., Pasqualone, D., Rougvie, A.E.,
Meyer, B.J., 2003. Chromosome cohesion is regulated by a clock gene
parologue *TIM-1*. *Nature* 423, 1002–1009.

Dark, J., 2005. Annual lipid cycles in hibernators: integration of physiology and
behavior. *Annu. Rev. Nutr.* 25, 469–497.

Dunlap, J.C., 1999. Molecular bases for circadian clocks. *Cell* 96, 271–290.

Fu, L., Pelicano, H., Liu, J., Huang, P., Lee, C., 2002. The circadian gene
Period2 plays an important role in tumor suppression and DNA damage
response in vivo. *Cell* 111 (7), 1055.

Gooley, J.J., Schomer, A., Saper, C.B., 2006. The dorsomedial hypothalamic
nucleus is critical for the expression of food-entrainable circadian rhythms.
Nat. Neurosci. 9, 300–302.

Gorbacheva, U.Y., Kondratov, R.V., Zhang, R., Cherukuri, S., Gudkov, A.V.,
Takahashi, J.S., Antoch, M.P., 2005. Circadian sensitivity to the chemother-
apeutic agent cyclophosphamide depends on the functional status of the
CLOCK/BMAL1 transactivation complex. *Proc. Natl. Acad. Sci. U.S.A.*
102 (9), 3407–3412.

Hagiwara, S.Y., Bolige, A., Zhang, Y., Takahashi, M., Yamagishi, A., Goto, K.,
2002. Circadian gating of photoinduction of commitment to cell-cycle
transitions in relation to photoperiodic control of cell reproduction in
Euglena. *Photochem. Photobiol.* 76 (1), 105–115.

Hamprecht, B., Nussler, C., Lynen, F., 1969. Rhythmic changes of hydroxy-
methylglutaryl coenzyme A reductase activity in livers of fed and fasted
rats. *FEBS Lett.* 4, 117–121.

Hastings, M.H., 1997. Circadian clocks. *Curr. Biol.* 7, R670–R672.

Hirayama, J., Luca, C., Doi, M., Paolo S-Colsi, 2005. Common pathways in
circadian and cell cycle clocks: light-dependent activation of *Fos/AP-1* in
zebrafish controls *CRY-1a* and *WEE-1*. *PNAS* 102.29, 10194–10199.

Itaka, C., Miyazaki, K., Akaike, T., Ishida, N., 2005. A role for glycogen
synthase kinase-3β in the mammalian circadian clock. *J. Biol. Chem.* 280
(33), 29397–29402.

Ishida, N.A., Mutoh, T., Ueyama, T., Bando, H., Masuibuchi, S., Nakahara, D.,
Tsujimoto, G., Okamura, H., 2005. Light activates the adrenal gland: timing
of gene expression and glucocorticoid release. *Cell Metab.* 2, 297–307.

Ishida, N., Kaneko, M., Allada, R., 1999. Biological clocks. *Proc. Natl. Acad.*
Sci. U.S.A. 96, 8819–8820.

Ishida, N., Miyazaki, K., Sakai, T., 2001. Circadian rhythm biochemistry: from
protein degradation to sleep and mating. *BBRC* 286, 1–5.

Jurevics, H., Hostettler, J., Barrett, C., Morell, P., Toews, A.D., 2000. Diurnal
and dietary-induced changes in cholesterol synthesis correlate with levels of
mRNA for HMG-CoA reductase. *J. Lipid Res.* 41, 1048–1054.

Kawasaki, H., Komai, K., Nakamura, M., Yamamoto, E., Ouyang, Z., Nak-
shima, T., Morisawa, T., Hashimoto, A., Shiozawa, K., Ishikawa, H.,
et al., 2003. Human *wee1* kinase is directly transactivated by and increased
in association with *c-Fos/AP-1*: rheumatoid synovial cells overexpressing
these genes go into aberrant mitosis. *Oncogene* 22, 6839–6844.

Keziban, U.-K., Mullen, T.E., William, K.K., Aziz, S., 2005. Coupling of
human circadian and cell cycles by the *Timeless* protein. *Mol. Cell. Biol.* 25
(8), 3109–3116.

Koike, N., Hida, A., Numano, R., Hirose, M., Sakai, Y., Tei, H., 1998.
Identification of the mammalian homologues of the *Drosophila* *timeless*
gene. *FEBS Lett.* 441, 427–431.

Kobayashi, H., Oishi, K., Hanai, S., Ishida, N., 2004. Effect of feeding
on peripheral circadian rhythms and behaviour in mammals. *Gene Cells*
9, 857–864.

Koyanagi, S., Kuramoto, Y., Nakagawa, H., Aramaki, H., Ohdo, S., Soeda, S.,
Shimeno, H., 2003. A molecular mechanism regulating circadian expres-
sion of vascular endothelial growth factor in tumor cells. *Cancer Res.* 63,
7277–7283.

Li, Z., Stuart, R.O., Quao, J., Pavlova, A., Bush, K.T., Pohl, M., Sakurai, H.,
Nigam, S.K., 2000. A role for *Timeless* in epithelial morphogenesis
during kidney development. *Proc. Natl. Acad. Sci. U.S.A.* 97, 10038–
10043.

565 Lowrey, P., Takahashi, J.S., 2004. Mammalian circadian biology: elucidating 612 genome-wide levels of temporal organization. *Annu. Rev. Genom. Hum. 613 Genet.* 5, 407–441.

566 Matsuo, T., Yamaguchi, S., Mitsui, S., Emi, A., Shimoda, F., Okamura, H., 614 2003. Control mechanism of the circadian clock for timing of cell division 615 in vivo. *Science* 302, 255–259.

567 Miyazaki, K., Nagase, T., Mesaki, M., Narukawa, J., Ohara, O., Ishida, N., 616 2004. Phosphorylation of clock protein PER1 regulates its circadian degra- 617 dation in normal human fibroblasts. *Biochem. J.* 380, 95–103.

574 Nagoshi, E., Saini, C., Bauer, C., Laroche, T., Naef, F., Schibler, U., 2004. 618 Circadian gene expression in individual fibroblasts: cell-autonomous and 619 self-sustained oscillators pass time to daughter cells. *Cell* 119, 693–705.

575 Nakagawa, H., Koyanagi, S., Takiguchi, T., Kuramoto, Y., Soeda, S., Shimeno, 620 H., Higuchi, S., Ohdo, S., 2004. 24-hour oscillation of mouse methionine 621 aminopeptidase2, a regulator of tumor progression, is regulated by clock 622 gene proteins. *Cancer Res.* 64 (22), 8328–8333.

581 Noguchi, E., Noguchi, C., Du, L.L., Russell, P., 2003. Swi1 prevents replication 623 fork collapse and controls checkpoint kinase Cds1. *Mol. Cell. Biol.* 23, 624 7861–7874.

582 Nyberg, K., Michelson, A.R.J., Putnam, C.W., Weinert, T.A., 2002. Toward 625 maintaining the genome: DNA damage and replication checkpoints. *Annu. 626 Rev. Genet.* 36, 617–656.

587 Ochi, M., Sono, S., Sei, H., Oishi, K., Kobayashi, H., Morita, Y., Ishida, N., 627 2003. Sex difference in circadian period of body temperature in Clock 628 mutant mice with Jcl/ICR background. *Neurosci. Lett.* 347, 163–166.

590 Oishi, K., Miyazaki, K., Ishida, N., 2002. Functional CLOCK is not involved in 629 the entrainment of peripheral clocks to the restricted feeding: entrainable 630 expression of mPer2 and BMAL1 mRNAs in the heart of Clock mutant mice 631 on Jcl:ICR background. *BBRC* 298, 198–202.

594 Oishi, K., Miyazaki, K., Kadota, K., Kikuno, R., Nagase, T., Atsumi, G., 632 Ohkura, N., Azama, T., Messaki, M., Yukimasa, S., Kobayashi, H., Ittaka, 633 C., Umehara, T., Horikoshi, M., Kudo, T., Shimizu, Y., Yano, M., Monden, 634 M., Machida, K., Matsuda, J., Horie, S., Todo, T., Ishida, N., 2003. Genome- 635 wide expression analysis of mouse liver reveals CLOCK-regulated circadian 636 output genes. *J. Biol. Chem.* 278 (42), 41519–41527.

600 Oishi, K., Amagai, N., Shirai, H., Kadota, K., Ohkura, N., Ishida, N., 2005a. 637 Genome-wide expression analysis reveals 100 adrenal gland-dependent 638 circadian genes in the mouse liver. *DNA Res.* 12, 191–202.

603 Oishi, K., Kobayashi, H., Hanai, S., Ishida, N., 2005b. CLOCK is involved in 639 the circadian transactivation of peroxisome-proliferator-activated receptor 640 α (PPAR α) in mice. *Biochem. J.* 386, 575–581.

606 Oishi, K., Atsumi, G., Sugiyama, S., Kodomari, I., Kasamatsu, M., Machida, K., 641 Ishida, N., 2006a. Disrupted fat absorption attenuates obesity induced by a 642 high-fat diet in Clock mutant mice. *FEBS Lett.* 580, 127–13030.

609 Oishi, K., Ohkura, N., Wakabayashi, M., Shirai, H., Atsumi, G., Sato, K., 643 Matsuda, J., Ishida, N., 2006b. CLOCK is involved in obesity-induced 644 disordered fibrinolysis in ob/ob mice by regulating PAI-1 gene expression. *J. 645 Thromb. Haemost.* 4 (8), 1774–1780.

565 Oishi, K., Ohkura, N., Kadota, K., Kasamatsu, M., Shibukawa, K., Machida, K., 645 Matsuda, J., Horie, S., Ishida, N., 2006c. Clock mutation affects the 646 circadian regulation of numbers of peripheral circulating blood cells. *J. 647 Circadian Rhythm*, in press.

567 Park, H., Sternglanz, R., 1999. Identification and characterization of the genes 648 for two topoisomerase I-interacting proteins from *Saccharomyces cerevi- 649 siae*. *Yeast* 15, 35–41.

574 Patel, D.D., Knight, B.L., Wiggins, D., Humphreys, S.M., Gibbons, G.F., 2001. 650 Disturbances in the normal regulation of SREBP-sensitive genes in PPAR 651 alpha-deficient mice. *J. Lipid Res.* 42 (3), 328–337.

575 Russell, P., Nurse, P., 1987. Negative regulation of mitosis by wee1, a gene 652 encoding a protein kinase homolog. *Cell* 49, 559–567.

577 Sakamoto, K., Nagase, T., Hukui, H., Horikawa, K., Okada, T., Tanaka, H., 653 Sato, K., Miyake, Y., Ohara, O., Kako, K., Ishida, N., 1998. Multitissue 654 circadian expression of rat period homolog (rPer2) mRNA is governed by 655 the mammalian circadian clock, the suprachiasmatic nucleus in the brain. *J. 656 Biol. Chem.* 273, 27039–27042.

581 Sakamoto, S., Miyazaki, K., Fukui, H., Oishi, K., Hayasaka, N., Okada, M., 657 Kamakura, M., Taniguchi, T., Nagai, K., Ishida, N., 2000. Molecular 658 characterization and nuclear localization of rat timeless-like gene product. 659 *BBRC* 279, 131–138.

582 Sangoram, A.M., Saez, L., Antoch, M.P., Gekakis, N., Staknis, D., Whiteley, 660 A., Fruechte, E.M., Vitaterna, M.H., Shimomura, K., King, D.P., Young, 661 M.W., Weitz, C.J., Takahashi, J.S., 1998. Mammalian circadian auto- 662 regulatory loop: a timeless ortholog and mPer1 interact and negatively 663 regulate CLOCK-BMAL1-induced transcription. *Neuron* 21, 1101– 664 1113.

587 Schibler, U., Sassone-corsi, P., 2002. A web of circadian pacemakers. *Cell* 111, 665 919–922.

590 Schibler, U., Juergen, R., Steven, A.B., 2003. Peripheral circadian oscillators in 666 mammals: time and food. *J. Biol. Rhythms* 18 (3), 250–260.

594 Shaw, P.J., Tononi, G., Greenspan, R.J., Robinson, D.F., 2002. Stress response 667 genes protect against lethal effects of sleep deprivation in *Drosophila*. 668 *Nature* 417 (6886), 287–291.

597 Turek, F.W., Joshu, C., Kohsaka, A., Lin, E., Ivanova, G., McDearmon, E., 669 Laposky, A., Losee-Olson, S., Easton, A., Jensen, D.R., Eckel, R.H., 670 Takahashi, J.S., Bass, J., 2005. Obesity and metabolic syndrome in circadian 671 Clock mutant mice. *Science* 308 (5724), 1043–1045.

600 You, S., Wood, P.A., Xiong, Y., Kobayashi, M., Du-Quiton, J., Hrushesky, W.J., 672 2005. Daily coordination of cancer growth and circadian clock gene 673 expression. *Breast Cancer Res. Treat.* 91 (1), 47–60.

603 Vitaterna, M.H., King, D.P., Chang, A.M., Kornhauser, J.M., Lowrey, P.L., 674 McDonald, J.D., Cove, W.F., Pinto, L.H., Turek, F.W., Takahashi, J.S., 1994. 675 Mutagenesis and mapping of a mouse gene, Clock, essential for circadian 676 behavior. *Science* 264, 719–725.

606 Zhang, J., Kaasik, K., Blackburn, M.R., Lee, C.C., 2006. Constant darkness 677 is a circadian metabolic signal in mammals. *Nature* 439 (7074), 678 340–343.

609



ELSEVIER

Journal of Alloys and Compounds 434–435 (2007) 718–720

Journal of
ALLOYS
AND COMPOUNDS

www.elsevier.com/locate/jallcom

Photocurrent of nanoassembled Si film in contact with electrolyte

S. Mamykin^{a,*}, A. Kasuya^a, A. Dmytruk^a, N. Ohuchi^b

^a *Center for Interdisciplinary Research, Tohoku University, Sendai 980-8578, Japan*

^b *Graduate School of Medicine, Tohoku University, Sendai 980-8579, Japan*

Available online 12 October 2006

Abstract

Nanoassembled Si thin films on conducting glass have been prepared. Films are photoactive and demonstrate “n-type” behavior in contact with electrolyte. Good correlation has been found between band gap obtained from luminescence and photocurrent. Up to such a small particle sizes the Si is still indirect optical material. Si nanoparticles demonstrate significantly reduced electron affinity 2.4 eV with much higher position of the bottom of conducting band compared to bulk Si while position of valence band did not change.

© 2006 Elsevier B.V. All rights reserved.

Keywords: Thin films; Electrode materials; Electronic band structure; Luminescence; Photocurrent

1. Introduction

Porous Si is a material of interest because of fundamental physical properties of quantum sized objects and possible promising applications in Si-based industry. Nanosized crystallites (<5 nm) have electrical and optical properties which are different from the bulk Si. Large specific surface area, increased band gap, luminescence in the visible region, changed electronic structure are basic properties used to design different devices such as solar cells with antireflecting coating [1], gas sensors, cold cathodes, flat panels, super capacitors, etc. [2,3]. It has also been proposed to use porous Si to improve hydrogen generation by p-Si in photoelectrolyses [4].

The usual way is to study porous Si on the Si wafer used for preparation. Unfortunately, in many cases, it is difficult to separate the properties of highly resistive, some times very thin layer of nanosized Si from the bulk material. The purpose of this report is to show a simple way to examine optical and photoelectrochemical properties of nanosized Si without influence of bulk Si. Prepared porous Si was separated from Si wafer and deposited as film on different substrate (conducting glass).

2. Experimental

Si nanoparticles were made by anodic etching of 0.12 Ω cm (100) p-type Si wafer with following dispersion of particles in toluen:ethanol (2:1) mixture

by ultrasonic bath. The piece of Si wafer of rectangular form with 2 cm width was immersed into electrolyte on depth of 5 mm. Anodic current was about 40 mA/cm² and processing time was 15 min. HF (46%):H₂O₂ (30%):methanol (97%) 3:3:1 mixture was used as electrolyte. After anodization and before ultrasonic bath, the porous Si was carefully rinsed by methanol. Films were prepared by electrophoretic deposition [6] of Si nanoparticles on conducting glass from suspension. Deposited films were calcinated at 150 °C in N₂ atmosphere. As prepared films have yellow color and demonstrate interference maxima and minima during transmittance measurements suggesting films uniformity. The thickness measured by SEM was about 1 μm (Fig. 1). Spectra of luminescence have been measured by Jusco FP-750 spectrophluorometer. Photoelectrochemical measurements were carried out in 0.1 M H₂SO₄ electrolyte. CHI440 potentiostat and three-electrode cell was used to record photocurrent. All potentials are versus Ag/AgCl₂ reference electrode. Thousand Watts Xenon lamp with monochromator was used as source of white and monochromatic light. Actual white light intensity was 60 mW/cm².

3. Results and discussion

Freshly prepared (dispersed in toluene:ethanol) Si nanoparticles show luminescence with peak at 2.28 eV (545 nm, Fig. 2). From luminescence maximum, the particle size can be estimated to be around ~2 nm [5]. Excitation spectrum (dashed curve in Fig. 2.) is proportional to absorption and can be used to estimate optical band gap which is about 2.5 eV.

Photoelectrochemical properties of films have been studied in 0.1 M H₂SO₄ electrolyte using three-electrode cell. Working electrode demonstrates different potentials in darkness and under white light (Fig. 3) at the open circuit conditions. This photovoltage is about 0.5 V and shows “n-type” behavior. It suggests more than 0.5 V band bending at the equilibrium. The polarity of the voltage says that photogenerated electrons go to substrate

* Corresponding author. Tel.: +81 22 795 57 58; fax: +81 22 795 57 50.
E-mail address: mamykin@cir.tohoku.ac.jp (S. Mamykin).

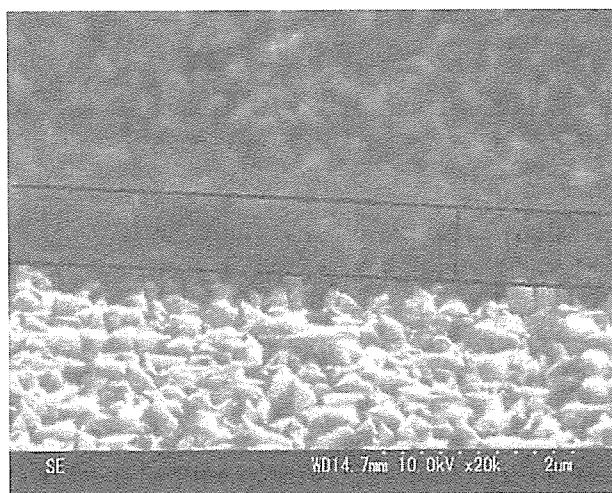


Fig. 1. SEM image of scratched and tilted sample. Si film thickness is about 1 μm .

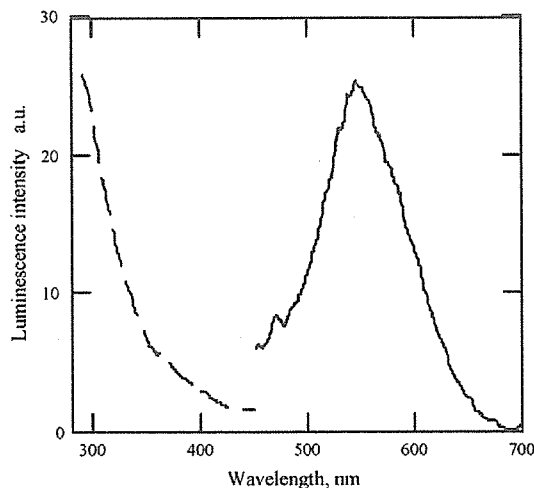


Fig. 2. Emission spectra (solid curve) and excitation (dashed curve) of luminescence of freshly prepared Si nanoparticles in toluene/ethanol mixture.

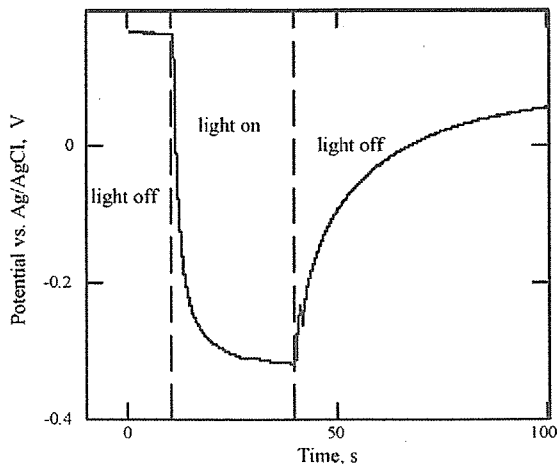


Fig. 3. Photopotential of sample vs. Ag/AgCl₂ reference electrode measured in 0.1 M H₂SO₄ electrolyte.

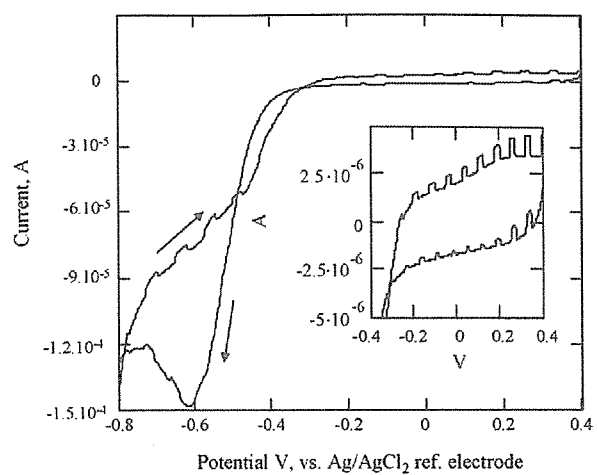


Fig. 4. Cyclic voltammetry under chopped white light of 60 mW/cm² intensity. The inset shows enlarged region of small current.

and holes go to contact with electrolyte. So, originally p-type Si was converted to n-type Si nanoparticles. This is in the agreement with high internal resistance of porous Si [2].

Cyclic voltammetry (Fig. 4) measured under chopped light allows to measure photo and dark current simultaneously. Significant dark current at negative potentials was present caused by reaction between substrate (fluorine doped SnO₂) and electrolyte. After dark current subtraction, the photocurrent (Fig. 5) shows three significant regions. The first is from 0.4 to -0.2 V. It increases from negative to positive potential with increasing of electric field in nanoparticles helping to separate photogenerated charge. This photocurrent is relatively small due to lack of hole scavenging at contact with electrolyte. Probably, the main holes consumer is oxidation reaction of Si. Second region is from -0.6 to -0.2 V. The photocurrent significantly increases due to increasing of reaction probability between generated holes and hydrogen. Third region is from -0.6 to negative side of potential. The photocurrent decreases with decreasing of electric field inside of Si particle at more negative potentials and riches zero at

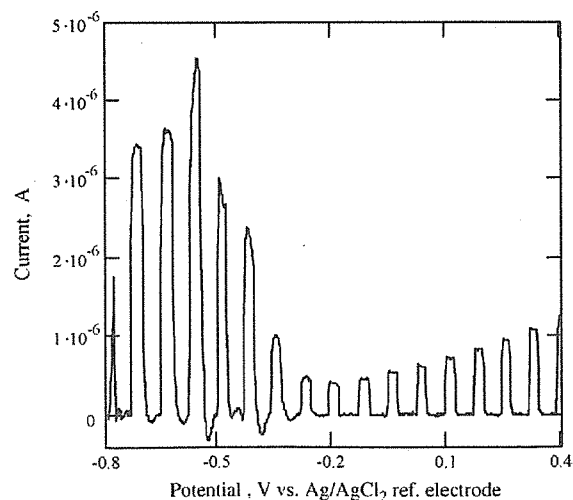


Fig. 5. Photocurrent of Si nanoparticles vs. applied potential.

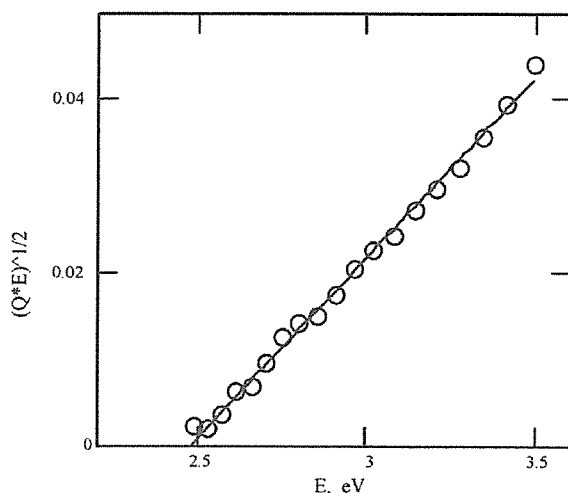


Fig. 6. Spectral dependence of quantum yield (Q) vs. photon energy. Special scale was applied to show indirect optical transitions. Measured optical band gap is 2.5 eV.

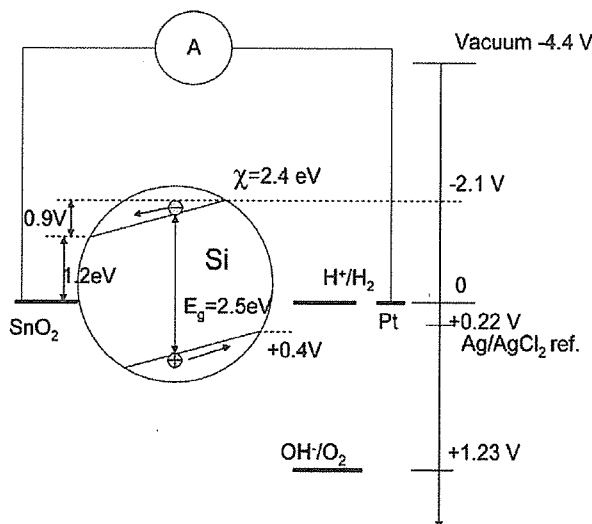


Fig. 7. Bands positions for Si nanoparticles in contact with electrolyte.

flat bands. Estimated flat band potential is about -0.9 V versus Ag/AgCl_2 reference electrode.

Spectral dependence of photocurrent was recorded at fixed applied bias ($+0.2$ V) where short circuit condition is performed.

Behavior of the photocurrent quantum yield (Q) versus photon energy (Fig. 6) demonstrates indirect band gap 2.48 eV. This is much higher than band gap of bulk Si (1.12 eV) due to quantum size effect.

On the basis of obtained band gap (2.48 eV) and flat band potential (-0.9 V) it is possible now to estimate the electron affinity χ and band positions of nanosized Si (Fig. 7). Taking into account the low concentrations of free carriers due to trap by surface states [2], the Fermi level is fixed at the middle of band gap. Summarizing, the flat band potential (-0.9 V) and distance between Fermi level and bottom of conduction band (-1.25 V), the position of conduction band against Ag/AgCl_2 is found to be -2.15 V. Valence band position can be found by subtracting the value of band gap (2.5 eV) and it is $+0.35$ V. Electron affinity as distance between bottom of conduction band and vacuum level can be found using potential of Ag/AgCl_2 in vacuum scale ($+4.6$ eV) and it is ~ 2.4 eV. This is significantly lower then for bulk Si (3.8 eV). It is interesting to mention that valence band position of bulk Si ($+0.4$ versus Ag/AgCl_2) is almost the same as in the case of nanosized Si.

4. Conclusions

Nanoassembled Si films on conducting glass are photoactive and demonstrate “n-type” behavior. Good correlation has been found between band gap obtained from luminescence and photocurrent. Up to such a small particle sizes, the Si is still an indirect optical material. Si nanoparticles demonstrate significantly reduced electron affinity 2.4 eV with much higher position of the bottom of conducting band compared to bulk Si while position of valence band did not change.

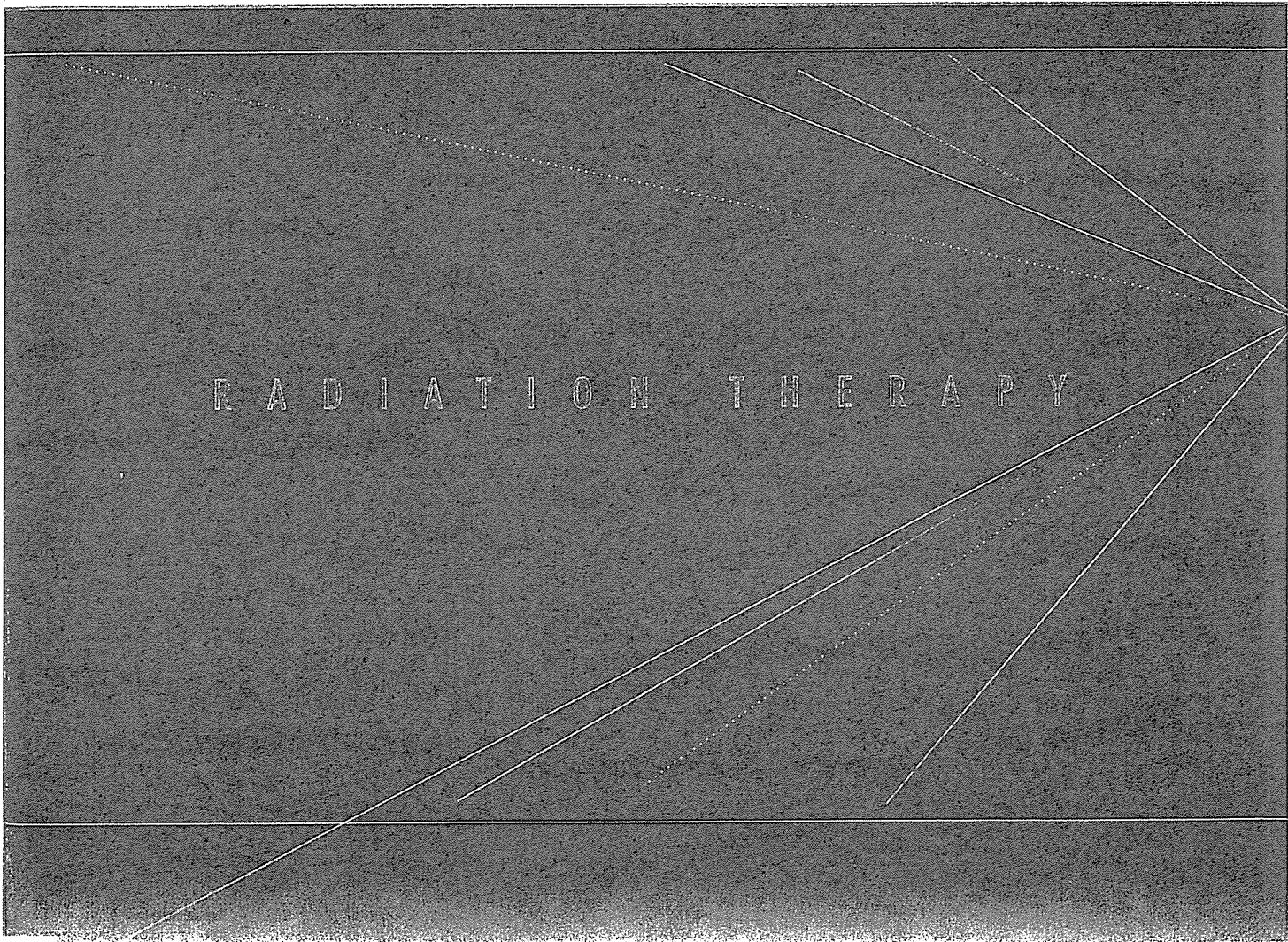
References

- [1] P. Menna, G. Di Francia, V. La Ferrara, *Solar Energy Mater. Solar Cells* 37 (1995) 13.
- [2] V. Lehmann, *Electrochemistry of Silicon*, Wiley-VCH/Verlag GmbH, Weinheim, 2002.
- [3] H. Foll, M. Christophersen, J. Carstensen, G. Hasse, *Mater. Sci. Eng. R* 39 (2002) 93.
- [4] N.R. Mathews, P.J. Sebastian, X. Mathew, V. Agarwal, *Int. J. Hydrogen Energy* 28 (2003) 629.
- [5] M.V. Wolkin, J. Jorne, P.M. Fauchet, G. Alan, C. Delerue, *Phys. Rev. Lett.* 82 (1999) 197.
- [6] H. Li, C. Xue, H. Zhang, C. Guo, C. Li, L. Chen, Z. Diao, *Int. J. Mod. Phys. B* 16 (2002) 4306.

早期のがん治療法の選択

放射線治療

編集 山田章吾



RADIATION THERAPY

金原出版株式会社

●執筆者

山田 章吾	東北大学大学院医学系研究科内科病態学講座放射線腫瘍学分野 教授
白土 博樹	北海道大学病院放射線科 助教授
藤田 勝久	北海道大学病院診療支援部放射線部門
石川 正純	北海道大学病院分子追跡放射線医療寄附研究部門 特任助教授
高井 良尋	東北大学医学部保健学科放射線治療技術学分野 教授
三津谷正俊	東北大学病院放射線部 副技師長
奈良崎覚太朗	東北大学病院放射線治療科
村上 昌雄	兵庫県立粒子線医療センター 医療部長
菱川 良夫	兵庫県立粒子線医療センター 院長
辻井 博彦	放射線医学総合研究所重粒子医科学センター センター長
大内 憲明	東北大学大学院医学系研究科外科病態学講座腫瘍外科学分野 教授
武田 元博	東北大学病院乳腺内分泌外科 助教授
石田 孝宣	東北大学病院乳腺内分泌外科 講師
芝本 雄太	名古屋市立大学大学院医学研究科量子放射線医学分野 教授
林 靖之	長崎大学医学部歯学部附属病院放射線科
中田 健生	市立札幌病院放射線科
晴山 雅人	札幌医科大学放射線医学 教授
坂田 耕一	札幌医科大学放射線医学 助教授
中村 和正	九州大学大学院医学研究院臨床放射線科学 講師
塩山 善之	九州大学大学院医学研究院臨床放射線科学
大賀 才路	九州大学大学院医学研究院臨床放射線科学
渋谷 均	東京医科歯科大学大学院医歯学総合研究科腫瘍放射線医学 教授
大西 洋	山梨大学大学院医学工学総合研究部放射線医学 助教授
淡河恵津世	久留米大学医学部放射線医学教室 講師
角藤 芳久	宮城県立がんセンター放射線科 医療部長
西村 恭昌	近畿大学医学部放射線医学教室放射線腫瘍学部門 教授
根本 建二	山形大学大学院医学系研究科放射線腫瘍学分野 教授
仲田 栄子	東北大学医学部保健学科診療放射線技術科学専攻
小野寺 浩	東北大学病院移植・再建・内視鏡外科